AN ABSTRACT OF THE THESIS OF

Kamal Issa Masoud Al-Malah for the Degree of Master of Science in Chemical Engineering Presented on February 7, 1991

Title: β-Lactoglobulin Adsorption Equilibrium at Low- and High-Energy Surfaces.

Redacted for Privacy

Abstract Approved _____

Joseph McGuire

Redacted for Privacy

Robert D. Sproull

Ellipsometry was used to study the effects of surface energetics and temperature on the equilibrium adsorptive behavior exhibited by β-lactoglobulin. β-Lactoglobulin isotherms at 25, 37, and 55°C were constructed for this purpose. The surfaces of acrylic, polycarbonate, polyester, glass, and #304 stainless steel were contacted with protein solutions of varying concentration, buffered at pH 6.7 with mono- and dibasic sodium phosphate. After three hours, the surfaces were mildly rinsed with deionized water and dried overnight. Optical properties of each film were ellipsometrically measured and the adsorbed mass was calculated as a function of film thickness and refractive index.

Contact angle methods were used to measure the hydrophobicity exhibited by each of the five solid surfaces. However, interpretation of protein adsorption results based solely on solid surface hydrophobicity proved unworkable. For polymers (low-energy surfaces),

the adsorbed mass of protein was explained with reference to the degree of extensibility of molecular structure. Glass (a high-energy surface) was observed to adsorb the greatest mass of β-lactoglobulin. Stainless steel was observed to adsorb the least mass of β-lactoglobulin and the plateau values of protein adsorption were found to be consistent with those reported elsewhere, and to lie within the range of adsorbed mass on metal surfaces in general.

The temperature dependence of β-lactoglobulin adsorption could not be clearly quantified. Apparently, any differences in adsorbed mass were too small to be detected by the instrument. In any event, other investigators have not detected any significant difference in adsorbed mass as long as the temperature was below the denaturation temperature of the protein.

β-Lactoglobulin Adsorption Equilibrium at Low- and High-Energy Surfaces

by

Kamal Issa Masoud Al-Malah

A THESIS

submitted to

Oregon State University

in partial fulfillment of
the requirement for the
degree of

Master of Science

Completed February 7, 1991

Commencement June 1991

APPROVED:

Redacted for Privacy

Assistant Professor of Bioresource Engineering, and Food Science & Technology in charge of major

Redacted for Privacy

Assistant Professor of Chemical Engineering in charge of major

Redacted for Privacy

Head of Department of Chemical Engineering

Redacted for Privacy

Dean of Graduate School

Date thesis is presented February 7, 1991

Typed by the researcher for Kamal Issa Masoud Al-Malah

ACKNOWLEDGEMENTS

In the Name of Allah, the Beneficent, the Merciful

I would like to express my gratitude to the **AICHE-RIFE** which funded the research for this project.

I would like to express my deep appreciation and thanks to both major advisors: **Dr. Joe. McGuire** and **Dr. R.D. Sproull**, for their guidance, encouragement, and in particular to his patience, Dr. McGuire, during the crisis and later the war in the ***Gulf of Ellipsometry***. More thanks to their unconditional help and support and to the **unconditional withdrawal** of the **UV-spectrophotometry** from the service.

A lot of thanks to the ***Protein Adsorption Allies:*** Sidney, Hamood, Viwat, Jingu Yang, and Burt. To them I say: we cherish the slogan: "we will fight till we liberate the last protein molecule from the solid surface".

Finally, **great thanks** to **my parents** for their **countless sacrifices and for their love.**

TABLE OF CONTENTS

APPENDICES

LIST OF FIGURES

LIST OF TABLES

LIST OF APPENDIX FIGURES

LIST OF APPENDIX TABLES

NOMENCLATURE

A	Area of interface (Appendix C.1).
a	A parameter in equation (3.11).
A_i	Partial molar area of the i^{th} component (Appendix C.1).
a_i	Activity coefficient of the i^{th} component (Appendix C.1).
A_p	Molar refractivity of protein [cm^3/mol].
$A_{ps(w)}$	A Hamaker constant [J].
b	An intercept as defined by equation (3.5) or as a parameter in equations (3.10) and (3.11).
Ceq	"Apparent" equilibrium concentration [mg/l].
C_i	Concentration of the i^{th} component (Appendix C.1)
C_p	Concentration of component p.
ΔC_p	Difference in heat capacity between the unfolded and folded states at constant pressure [kcal/mol K] (Appendix A).
C_q	Concentration of component q (Appendix B).
d	Film thickness [nm].
d_o	Equilibrium distance between protein and surface [m].
ΔE_p	Adsorption energy per polymer (Appendix C.1).
Δe_p	Adsorption energy per segment (Appendix C.1).
ΔE_s	Adsorption energy of surfactant (Appendix C.1).
F	Helmholtz free energy or Farady's constant (Appendix C.1).
f_i	Fugacity coefficient of the i^{th} component (Appendix C.1).
$\Delta F_{ps(w)}$	Change in free energy produced when protein and solid located

in water are brought from infinite to equilibrium distance [J/m^2].

G Gibbs free energy (Appendix C.1).

ΔH_o Enthalpy change at temperature T_o between the unfolded and folded states [kcal/mol] (Appendix A).

ΔH_T Enthalpy change at temperature T between the unfolded and folded states [kcal/mol] (Appendix A).

K Equilibrium constant (Appendix C.1).

k A slope as defined by equation (3.5), or the Boltzmann constant (Appendix C.1).

k_1 A rate constant (Appendix C.1).

k_2 A rate constant (Appendix C.1).

k_3 A rate constant (Appendix C.1).

k_4 A rate constant (Appendix C.1).

K_p Affinity constant of component p, or equilibrium constant.

K_q Affinity constant of component q (Appendix B).

K_s Equilibrium constant of surfactant.

k_s Conjugate part (or extinction coefficient) of refractive index.

M_p Molecular weight of protein [g/mol].

n_b Buffer refractive index.

n_f Film refractive index.

n_i Surface concentration [mol/unit area] of the i^{th} component (Appendix C.1).

n_s Real part of refractive index for substrate.

r_p Chain length of component p (Appendix B).

ΔS_o Entropy change at temperature T_o between the unfolded and folded states [kcal/mol K] (Appendix A).

ΔS_T Entropy change at temperature T between the unfolded and folded states [kcal/mol K] (Appendix A).

T Temperature.

T_o Reference temperature.

U Internal energy (Appendix C.1).

V_{20} Partial specific volume of protein at 20°C [cm^3/g].

V_i Partial molar volume of the i^{th} component (Appendix C.1).

W_a Work of adhesion [mJ/m^2], energy required to part unit area of liquid from a solid.

W_a^p Polar component of the work of adhesion [mJ/m^2].

X_i Mole fraction of the i^{th} component (Appendix C.1).

z_c Ionic charge of the counter ion (Appendix C.1).

z_p Molecular charge of protein (Appendix C.1).

Greek Symbols

Γ Adsorbed mass of protein [$\mu g/cm^2$].

γ Interfacial free energy (or interfacial tension) (Appendix C.1).

γ_L Liquid surface free energy [mJ/m^2] (or liquid surface tension [mN/m]).

γ_L^d Dispersive component of liquid surface tension [mJ/m^2].

γ_L^p Polar component of liquid surface tension [mJ/m^2].

Γ_{max} Plateau value of adsorbed mass [$\mu g/cm^2$].

γ_{pw} Interfacial free energy between protein and water [J/m^2].

γ_S Solid surface free energy [mJ/m^2] (or solid surface tension [mN/m]).

γ_S^d Dispersive component of solid surface tension [mJ/m^2].

γ_{SL} Interfacial free energy [mJ/m^2] (or interfacial tension [mN/m]).

γ_S^p Polar component of solid surface tension [mJ/m^2].

γ_{sp} Interfacial free energy between soild surface and protein [J/m^2].

γ_{sw} Interfacial free energy between soild surface and water [J/m^2].

Δ An angle, defined as a change in phase difference [°].

θ Contact angle in degrees [°], formed when a drop of liquid is in contact with a solid surface *or* $\theta = \theta_p + \theta_s$ (Appendix C.1).

θ_o Surface coverage (or fraction) of solvent (Appendix C.1).

θ_p Surface coverage (or fraction) of component p, *and* of polymer.

θ_q Surface coverage (or fraction) of component q (Appendix B).

θ_s Surface coverage (or fraction) of surfactant (Appendix C.1).

μ_i Electrochemical potential of the i^{th} species (Appendix C.1).

ν Number of cells of the surface layer occupied by one adsorbed polymer (Appendix C.1).

π_s Spreading pressure.

σ A constant that depends on the composition of the system (Appendix B).

ϕ_1 Electrostatic potential at the protein-liquid side interface (Appendix C.1).

ϕ^*_p Volume fraction of component p in the bulk solution (Appendix B).

ϕ^i_p Volume fraction of component p at the interface (Appendix B).

ϕ_o Volume fraction of the solvent in the bulk solution (Appendix C.1).

ϕ_m Electrostatic potential at the protein-surface interface (Appendix C.1).

ϕ_p Volume fraction of the polymer in the bulk solution (Appendix C.1).

ϕ_s Volume fraction of the surfactant in the bulk solution (Appendix C.1).

$\phi\zeta$ Electrostatic potential at the shear plane (Appendix C.1).

χ Flory-Huggin interaction parameter [unit of enthalpy/solvent molecule] (Appendix B).

χ_s A parameter to account for the interaction of a polymer segment with the surface [unit of enthalpy / solvent molecule] (Appendix B).

Ψ An angle, defined as the arctangent of the factor by which the amplitude ratio changes [°].

Subscripts

c	Counter ion (Appendix C.1).
p	Protein (Appendix C.1).
s	Solvent (Appendix C.1).
os	Standard state for solvent (Appendix C.1).
op	Standard state for protein (Appendix C.1).

Superscripts

m	Monolayer film (Appendix C.1).
′	Total system property (i.e., bulk plus surface phase) (Appendix C.1).
om	Standard state for the electrochemical potential of the i^{th} component in the monolayer film (Appendix C.1).

1. INTRODUCTION

1.1 Background

Interactions between proteins and surfaces are involved in problems commonly encountered in pharmaceutical and food industries, and such interactions can be associated with profound consequences in medicine as well. For instance, clinicians have studied plasma protein interactions with the surfaces of transplanted foreign devices and subsequent thrombosis, which are correlated with the biocompatibility of the device. Food and bioprocess engineers have carried out similar studies with the belief that protein adsorption, due to the heat sensitivity of proteins and their high content in some fluid foods, likely plays a major role in the fouling of membrane and heat exchange surfaces. Deposition of milk serum protein onto stainless steel surfaces of heat exchangers during thermal processing of milk has been well documented, and these proteins, β-lactoglobulin in particular, are the main components of type A deposit, i.e., soft, voluminous, and curd-like. Protein adsorption appears to mediate bacterial and spore adhesion as well, and a great deal of time, labor, energy, and money is required daily to clean these surfaces.

A great deal of effort has been devoted to studying the different factors that influence adsorption. The question of how these factors interact is undoubtedly complex, and a comprehensive model of protein

adsorption is not available. The important factors affecting adsorption can be classified under one or more of the following three areas:

1. protein characteristics: including isoelectric point, net charge and charge distribution, 3-D structure in solution, placement and nature of hydrophobic patches, and conformational variability;

2. surface properties: including topography and heterogeneity of the surface, surface potential, surface composition, water binding, and interfacial entropic effects; and

3. medium conditions: including solution pH, temperature, ionic strength, equilibrium concentration, hydrodynamics, and buffer type.

Adsorption of proteins involves attachment of multiple segments to the adsorbent surface. For each protein molecule that adsorbs, several solvent molecules are released from the solid surface and protein "surface" accompanied by a gain of entropy which in essence is translational. From this perspective, protein adsorption is entropically driven, particularly when hydrophobic interaction constitutes the prevalent binding mechanism.

Electrostatic interactions also strongly influence the pattern of protein adsorption. The tendency of protein adsorption to exhibit a maximum at or near the isoelectric point is usually explained with reference to electrostatics.

Experimental observations indicate that protein adsorption isotherms sometimes follow a Langmuir or Langmuir-type isotherm, where a steep initial slope over very low concentrations is followed by attainment of a plateau at higher concentrations. Another observation of importance is that protein adsorption is often an apparently

irreversible process. The adsorbed mass is observed to remain constant or only slightly decrease when the adsorbed protein film is brought into contact with a protein-free solution.

1.2 Objective and Method of Approach

The objective of this study was to better understand the effects of surface energetics and temperature on β-lactoglobulin adsorption equilibrium, as it is indicated by an isotherm. To construct the isotherms, the surfaces of glass, #304 stainless steel (SS), acrylic, polyester, and polycarbonate were contacted with buffered protein solutions with concentrations ranging from about 0.1 to 3.0 mg/ml, at pH 6.7. After three hours, the surfaces were mildly rinsed to remove less tenaciously bound protein, and dried. Ellipsometry was used to measure optical properties of the protein films, and the Lorentz-Lorenz relationship was used to calculate adsorbed mass as a function of ellipsometrically determined film thickness and refractive index.

2. LITERATURE REVIEW

A brief literature review is presented here. For further details and a more rigorous review, refer to Appendices A, B, and C.

2.1 Proteins

Proteins are biological macromolecules synthesized in cells for specific functions. They are high molecular weight polyamides that adopt exquisitely complex structures. This complexity in protein structure is characterized by different levels: primary, secondary, tertiary, and quaternary structure. Primary structure is described (1) by the amino acid sequence itself and the location of disulfide bonds (i.e., covalent connections within the protein molecule). Secondary structure describes the spatial arrangement of amino acid residues that are near one another in the linear sequence. An α-helix and β-sheet are typical examples of secondary structure. Tertiary structure defines the spatial arrangement of amino acid residues that are far apart in the linear sequence. If a protein has two or more polypeptide chains, each with its exclusive primary, secondary, and tertiary structure, such chains can associate to form a multi-chain quaternary structure. Hence, a quaternary structure refers to the spatial arrangement of such subunits and their interaction.

Protein molecules are stabilized by different intramolecular forces that play a key role in maintaining protein structure. In addition to the planar peptide bond that constitutes the backbone of the

molecule, there are intramolecular forces, though smaller in magnitude than a covalent bond, that are as important as the peptide bond itself. These intramolecular interactions include disulfide linkages, hydrophobic bonding, hydrogen bonding, dispersion forces, and electrostatic forces. The disulfide covalent bonds are thought (2) to stabilize proteins by reducing the conformational entropy of the unfolded chain. Hydrophobic interactions (3) are basically entropically driven, largely due to order/disorder phenomena in the surrounding water. Hydrogen bonding forces are considered to be one of the major contributors to the largely temperature-independent part of the enthalpy of stabilization. Hydrogen bonds are very common in proteins and are partly responsible for the α-helix and β-sheet stabilities. The importance of dispersion or van der Waals forces for protein stability hinges on differences in packing in the folded and unfolded states (2). Proteins may be considered polyelectrolytes since ionizable groups from amino acid side chains and terminal amino acids participate in an acid-base equilibrium. Ionizable groups are not generally distributed randomly over protein surfaces, reflecting their individual structural and functional roles.

2.2 Adsorption

Adsorption involves migration of a substance from one phase to the surface of an adjacent phase, accompanied by its accumulation at the interface (4). Adsorption is a result of the binding forces between individual atoms, ions or molecules of an adsorbate and the adsorbent

surface. These binding forces or interactions vary in magnitude from the weak van der Waals type of binding (i.e., physical adsorption) to the strong covalent type of binding (i.e., chemisorption). Polymer adsorption in general and biopolymer adsorption in particular show a range of binding energies depending on the type of forces involved in adsorption. Polymer adsorption differs drastically from that of small molecules. This is basically due to the large number of conformations that a macromolecule can have, both in the bulk of a solution and at the interface. The entropy loss or gain associated with a given flexible polymer can be greater than that for small molecules or relatively stiff molecules (5).

2.3 Protein Adsorption

Surveying the literature, one can recognize that protein behavior at interfaces is a controversial issue. Keeping this in mind, some pertinent literature will be briefly reviewed based on the author's own conclusions.

A thermodynamic approach was proposed by De Feijter et al. (6) to explain the adsorption of nonionic, flexible polymers. Their approach relies on a pseudo-lattice model which led them to conclude that the adsorption isotherm of the polymer exhibits a high affinity character; in other words, high adsorption at very low bulk concentration with a plateau almost over the entire range (see Appendix C, Figure C.1). This approach is also expected to apply to proteins, even though they are considered to be somewhat rigid structures with some net charge.

Levine (7) studied the thermodynamics of adsorbed protein films. He expressed the enrichment factor (see Appendix C, equation C.34) of the film by protein as a function of surface energetics and electrostatics. He suggested that materials with high surface energy are expected to adsorb more than those of low surface energy. The role of electrostatic charge in either enhancing or minimizing adsorption from an electrostatic barrier point of view was also emphasized.

Horbett (8) studied the adsorption of plasma proteins at polyethylene, surface-grafted with methacrylate derivatives, using an I-125 radiolabelling technique. He found that for hemoglobin the adsorbed amount generally increased with time, and varied from one surface to another. The adsorbed amount was observed to increase with increasing surface hydrophobicity. The low rate of adsorption of hemoglobin to surfaces from plasma led Horbett to suggest that this may be due to multilayer formation, enzymatic cross linking, interfacial aggregation, configurational rearrangements, or chemical alterations in the adsorbing species. De Feijter et al. (9) suggested a multilayer formation and a conformational rearrangement of the adsorbed molecule, when they studied the adsorption behavior of κ-casein at the air-water interface using ellipsometry. Brash and Lyman (10) studied adsorption of plasma proteins in solution to uncharged, hydrophobic polymer surfaces using infrared internal reflection spectroscopy. In general, the plateau values indicated a monolayer formation of protein at the surfaces, with the exception of γ-globulin on polydimethyl-siloxane, which exhibited a more compact layer because of the high surface concentration.

Lee and Ruckenstein (11) studied the adsorption of proteins onto polymeric surfaces of different hydrophilicities. They observed that the most hydrophobic surface exhibited an adsorbed mass smaller than either of the less or intermediate hydrophobic surfaces. The most hydrophilic surface, which was glass in their study, exhibited an adsorbed mass larger than the most hydrophobic surface.

Baier (12) investigated the initial events associated with interactions of blood with a foreign surface. Upon applying extraction to the one-minute film, the CH_2 (i.e., hydrocarbon groups) absorption band vanished, and the free carbonyl (i.e., fatty acid type material) band disappeared completely. The protein bands remained, suggesting an irreversible adsorption associated with protein conformational rearrangement. It was only after mechanical scrubbing using a soft brush accompanied by an aqueous detergent solution, that the multiple attenuated internal reflection infrared spectroscopy spectrum indicated a completely clean substrate, as also indicated from contact angle measurements.

Arnebrant et al. (13) studied the temperature dependence of adsorption for α-lactalbumin and β-lactoglobulin on chromium surfaces. They observed that the curves for β-lactoglobulin at 25, 66, 70, and 73°C were rather similar. It was only when the temperature exceeded the denaturation temperature (79°C) of β-lactoglobulin, that they could observe a significant difference in the adsorbed mass.

In summary, protein adsorption exhibits a diversity in behavior from one surface to another. This diversity results from the complexity of the protein structure itself and from the many variables on which

protein adsorption depends. Nevertheless, the interfacial phenomena can be explained in terms of surface effects, in general, including surface energetics, composition, morphology, and hydrophobic-hydrophilic balance.

3. MATERIALS AND METHODS

3.1 Materials

Five sample plates (approximately 1 cm X 2 cm) were constructed from each of five different materials: #304 stainless steel (Engineering Machine Shop, OSU, Corvallis, OR), glass (Erie Scientific Co., Portsmouth, N.H.), polycarbonate, polyester, and acrylic (Sheffield Plastics, Inc., Sheffield, MA). The surfaces of the polymers were protected during shipment from the supplier and storage with a protective polymeric film applied by the manufacturer. The #304 stainless steel was polished to a mirror finish. All sample plates were immersed in deionized water with ultrasonic treatment for 10 minutes, rinsed with deionized water and dried at room temperature in a dessicator prior to use.

Each of the polymers as well as glass are transparent. During ellipsometric analysis, to prevent reflection of the laser beam from the "back" of these materials (*i*.e., the surface opposite that being analyzed), one side of each was blackened evenly with a vinyl plastic color spray (New York Bronze Powder Co. Inc.). Substrate constants (refractive indices of the bare surfaces, required for ellipsometric evaluation of film thickness and refractive index) of each plate were then determined with ellipsometry and are shown in Table 3.1.

Table 3.1 The substrate index of each material used (their associated standard errors shown in parentheses). $N_S = n_S - k_S\, i$ where n_S is the real part of refractive index for substrate, and k_S is the conjugate part (or extinction coefficient) of refractive index for substrate.

Surface	n_S	k_S
Glass	1.514 (0.005)	0.008 (0.005)
#304 SS	2.762 (0.041)	4.195 (0.036)
Acrylic	1.486 (0.001)	0.007 (0.001)
Polyester	1.562 (0.005)	0.010 (0.002)
Polycarbonate	1.574 (0.001)	0.007 (0.002)

3.2 Surface Characterization

A contact angle technique (i.e., goniometry) was used to measure the hydrophobicity of each of the five material surfaces. The technique basically relies on attaining an equilibrium between a drop of a test liquid and the surface to be examined. A force balance performed on a drop of liquid at equilibrium on a plane surface is known as Young's equation. Written in its simplest form:

$$\gamma_S = \gamma_{SL} + \gamma_L \cos\theta \qquad (3.1)$$

where γ_S is the solid surface free energy [mJ/m^2] (or solid surface tension [mN/m]); γ_{SL} is the interfacial free energy [mJ/m^2] (or interfacial tension [mN/m]); γ_L is the liquid surface free energy

[mJ/m^2] (or liquid surface tension [mN/m]); and θ is the contact angle, in degrees [°], formed when a drop of liquid is in contact with a solid surface.

The work of adhesion, W_a [mJ/m^2], is the energy required to part unit area of liquid from a solid. It is defined by the Dupre' equation (an energy balance):

$$W_a = \gamma_S + \gamma_L - \gamma_{SL} \quad (3.2)$$

Combining the Young and Dupre' equations yields:

$$W_a = \gamma_L (1 + \cos \theta) \quad (3.3)$$

The concept of resolving solid and liquid surface tension into additive polar and dispersive components is rather well developed. Application of this concept to characterization of food contact surfaces has been fully described elsewhere (14). A brief summary is presented here.

With test liquids for which liquid surface tension, γ_L, the dispersive component of liquid surface tension, γ_L^d, and the polar component of liquid surface tension, γ_L^p, ($\gamma_L = \gamma_L^d + \gamma_L^p$), and with methodology (14) for evaluation of the dispersive component of solid surface tension, γ_S^d, the polar component of the work of adhesion, W_a^p, can be calculated as follows:

$$W_a^p = \gamma_L(1+ \cos \theta) - 2(\gamma_L^d \gamma_S^d)^{1/2} \quad (3.4)$$

Equation (3.4) can be used to evaluate W_a^p for each test liquid contacted with a given material. Since γ_L^p is known for each test liquid (ethanol-water solutions of 0, 10, 20, 30, and 40% (v/v) ethanol were used as the test liquids), a plot of W_a^p vs. γ_L^p can be constructed. Such a plot reveals a unique relationship between W_a^p and

γ_L^P for each material as a result of differences in γ_S^P. This relationship is usually found to be linear, i.e.:

$$W_a^P = k\,\gamma_L^P + b \qquad (3.5)$$

The slope, k, which varies from one surface to another, is an indirect measurement for the the polar component of solid surface energy, γ_S^P, and was found (14) to be independent of the diagnostic liquid used. The value of the intercept, b, could be interpreted as a measure of π_s, the reduction in surface energy of the solid resulting from adsorption of vapor from the diagnostic liquid.

The value of the polar component of the work of adhesion between any given solid surface and water ($W_a^P{}_{water}$) can be defined in a similar fashion as:

$$W_a^P{}_{water} = k(\gamma_L^P{}_{water}) + b \qquad (3.6)$$

$W_a^P{}_{water}$ can be used (15) as an indication for surface hydrophilicity; since it can be calculated with equation (3.6), actual contact angle data for water need not be used. This avoids rather serious problems associated with using pure water as a diagnostic liquid. The parameters k, b and $W_a^P{}_{water}$ were recorded for each surface under investigation.

3.3 Adsorption

The five sample plates of each material were first equilibrated with 300 ml of sodium phosphate buffer (using both mono- and dibasic sodium phosphate; pH = 6.7) at the desired temperature (25, 37, or 55°C), then contacted with 300 ml fresh, buffered β-lactoglobulin solution at the same temperature and of the desired concentration, for 3

hours with agitation (100 rpm, using an orbital shaker, Model 2001, Lab-Line Instruments, Inc., Melrose park, IL). Solution concentrations ranged from about 0.1 to 3.0 mg/ml. Equilibration with buffer as well as with protein were both attained in the constant temperature orbital shaker. The surfaces were subsequently rinsed for one minute in 300 ml distilled water with stirring (magnetic stirrer set at #2), and dried overnight in a dessicator. Mild rinsing was applied here for the sake of removing less tenaciously bound protein.

The thickness and refractive index of the film formed on each surface were ellipsometrically determined. In each case, multiple readings were made at each of approximately ten different surface locations at 25°C, and 30 different surface locations at both 37 and 55°C. Ellipsometric measurements were made using an automated ellipsometer (Model L104B-IBM 25, Gaertner Scientific Corp., Chicago, IL). Ellipsometry is an optical technique used to determine the thickness and refractive index of thin films. Basically, a laser beam of known physical properties is transmitted to a film-covered surface and reflected. Physical properties of the beam change upon reflection, and these changes are measured. The measured differences between the properties of the incident and reflected beams are totally dependent on film thickness and refractive index; these film properties are evaluated using software written in our laboratory. Given the values of film thickness and refractive index, adsorbed mass of a film immersed in buffer can be calculated by the following Lorentz-Lorenz relationship, as experimentally verified by Cuypers et al. (16):

$$\Gamma = 0.3\, d\, f(n)\, (n_f - n_b) / [(A_p/M_p) - V_{20}(n_b^2 - 1)/(n_b^2 + 2)] \qquad (3.7)$$

where

$$f(n) = (n_f + n_b)/[(n_f^2 + 2)(n_b^2 + 2)] \quad (3.8)$$

Γ [$\mu g/cm^2$] is the adsorbed mass of protein; d [nm] is the film thickness; A_p [$cm^3\ mol^{-1}$] is the molar refractivity of protein; M_p [$g\ mol^{-1}$] is the molecular weight of protein; and V_{20} [$cm^3\ g^{-1}$] is the partial specific volume of protein at 20°C. The refractive indices n_f and n_b refer to that of the entire "mixed" film and of pure buffer, respectively. M/A ratio has been tabulated for common amino acids, therefore M/A for any protein molecule can be calculated by appropriately summing the M/A ratio for each of its amino acids. For β-lactoglobulin, a value of 4.1 for M_p/A_p ratio was used (13).

If a protein film remaining on a surface after rinsing is dried, the adsorbed layer can then be referred to as a mixed layer consisting of protein and air. In this case $n_b = n_{air} = 1.000$, and equation (3.7) simplifies to:

$$\Gamma = 0.1\ d\ (M_p/A_p)\ (n_f^2 - 1)/(n_f^2 + 2) \quad (3.9)$$

All raw ellipsometric data (Ψ and Δ) and computer output including refractive index, film thickness, and adsorbed mass calculated by the Lorentz-Lorenz equation, were stored on a diskette for later analysis.

3.4 Construction of Adsorption Isotherms

The relationship between adsorbed mass of protein and its equilibrium concentration may be described by more than one model or equation. Usually, the adsorbed mass is observed to either eventually level off (i.e., follow the Langmuir or a Langmuir-type model) or to

continuously increases with equilibrium concentration (i.e., the Freundlich model). A Langmuir-type model of the form

$$\Gamma = \Gamma_{max} C_{eq} / (b + C_{eq}) \quad (3.10)$$

can be used to describe β-lactoglobulin adsorption at each surface, where C_{eq} is the apparent equilibrium concentration [mg/l]; Γ_{max} is the plateau value; and b [mg/l] is a constant such that Γ_{max}/b is the initial slope of a plot of Γ versus the apparent equilibrium concentration. The Langmuir model assumes a monolayer film, a homogeneous surface, and no lateral interaction among adsorbed protein molecules. Although features of equation (3.10) resemble that of the Langmuir isotherm, it should not be taken to imply or assume any of its fundamental premises.

The Freundlich model, which is of the form

$$\Gamma = a(Ceq)^b \quad (3.11)$$

was also used in parallel with the Langmuir-type model to describe β-lactoglobulin adsorption. The constants a and b in equation (3.11) are function constants that define the functionality of Γ versus the apparent equilibrium concentration, C_{eq}. The Freundlich model has no theoretical foundation, but is empirical. A plot of Γ versus equilibrium concentration does not exhibit a plateau value, but increases monotonically.

4. RESULTS

Plots of the normalized adsorbed mass versus normalized, apparent equilibrium concentration for the five materials at 25, 37, and 55°C are shown in Figures 4.1, 4.2, and 4.3, respectively. In all figures shown, the following abbreviations were used to designate each type of material: acrylic (AC); glass (GS); polycarbonate (PC); polyester (PE); and #304 stainless steel (SS). The term "apparent equilibrium" was used to indicate that values of protein concentration recorded were probably not true equilibrium values. Andrade(3) indicated that true equilibrium may not be attained within the adsorption period of an experiment. One should also expect that adsorption onto the container surfaces as well as air/water interfacial effects are present and can not be prevented; however these effects on the plateau value were found to be negligible, and the initial concentration was used to represent an apparent equilibrium value. Normalization was made such that each value of apparent equilibrium concentration (in mg/l) was divided by 4000 mg/l (the upper limit of the concentration range). All values of adsorbed mass (in $\mu g/cm^2$) were divided by 4 $\mu g/cm^2$ (the upper limit of adsorbed mass observed). For each adsorption isotherm constructed, the regressed parameters of the Langmuir-type model (equation 3.10), and their associated standard errors, are listed in Table 4.1.

In order to compare adsorbed mass observed among the materials at each temperature, the regressed isotherms for the five materials together are shown in Figures 4.4, 4.5, and 4.6.

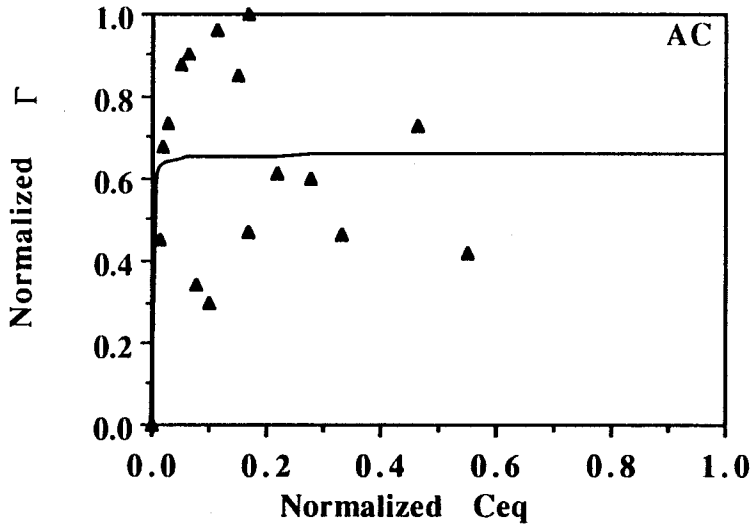

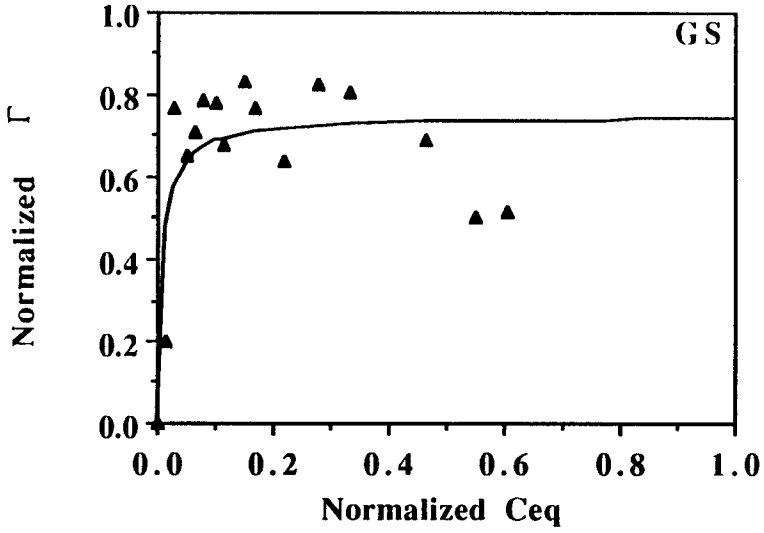

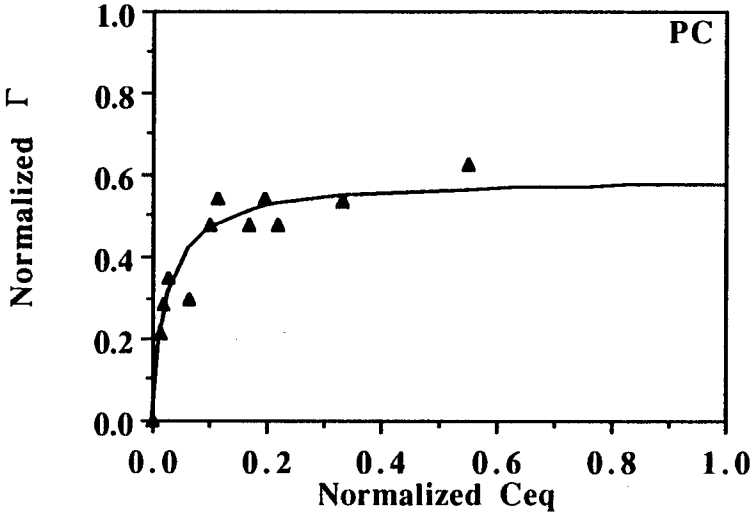

Figure 4.1

Experimentally measured adsorption data fit to the Langmuir-type isotherm for each material at 25°C.

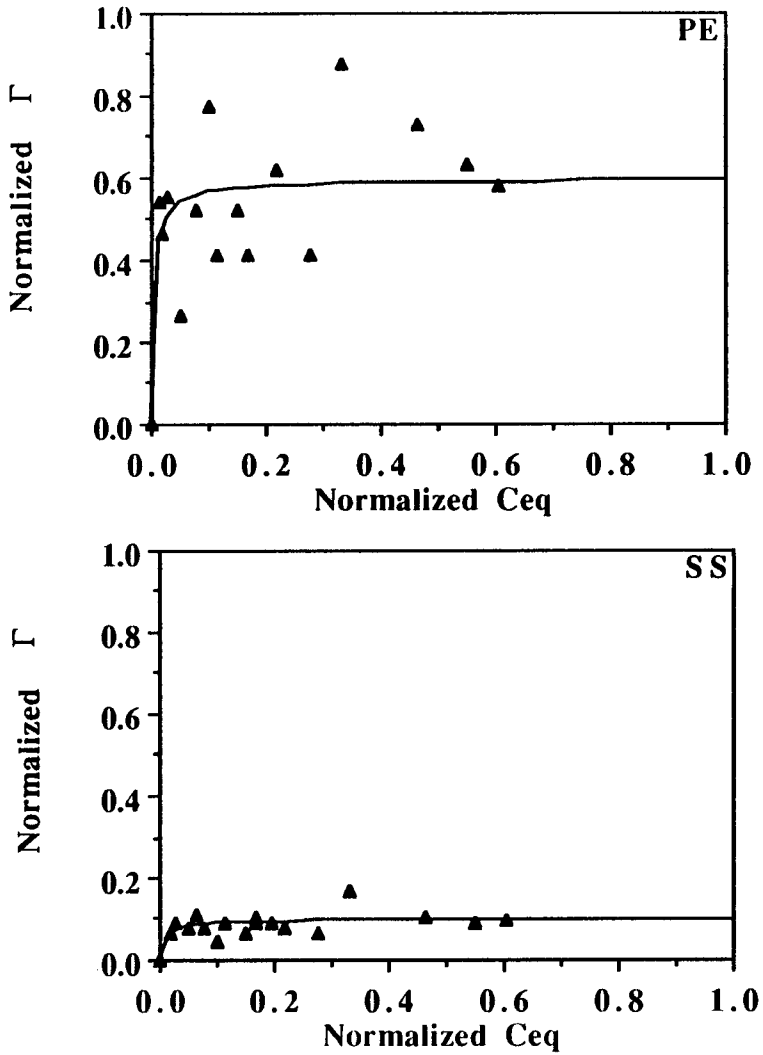

Figure 4.1 (continued)

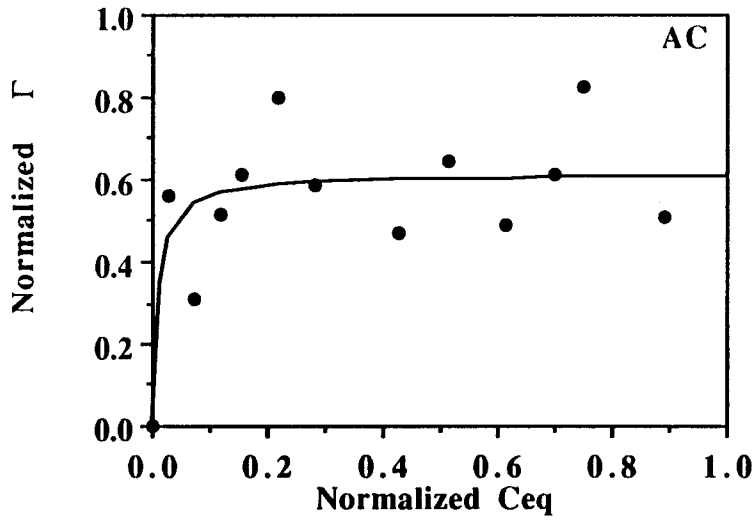

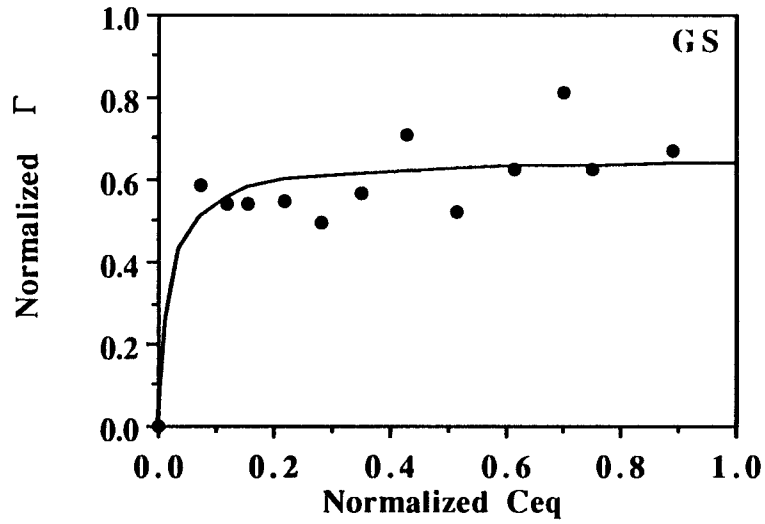

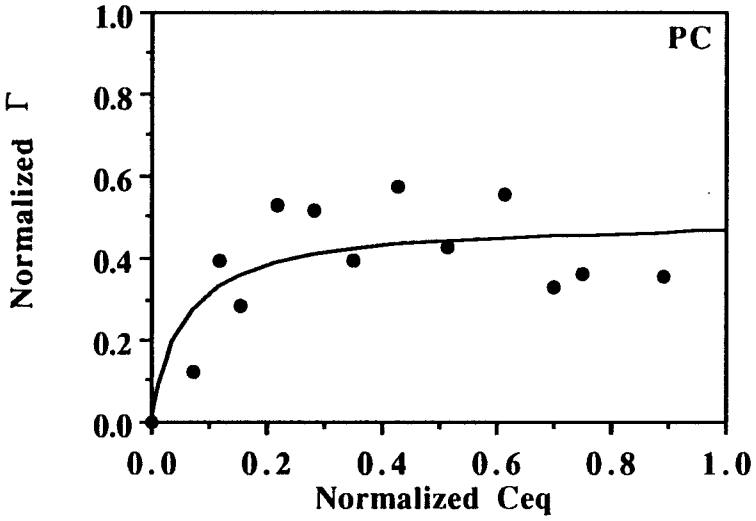

Figure 4.2

Experimentally measured adsorption data fit to the Langmuir-type isotherm for each material at 37°C.

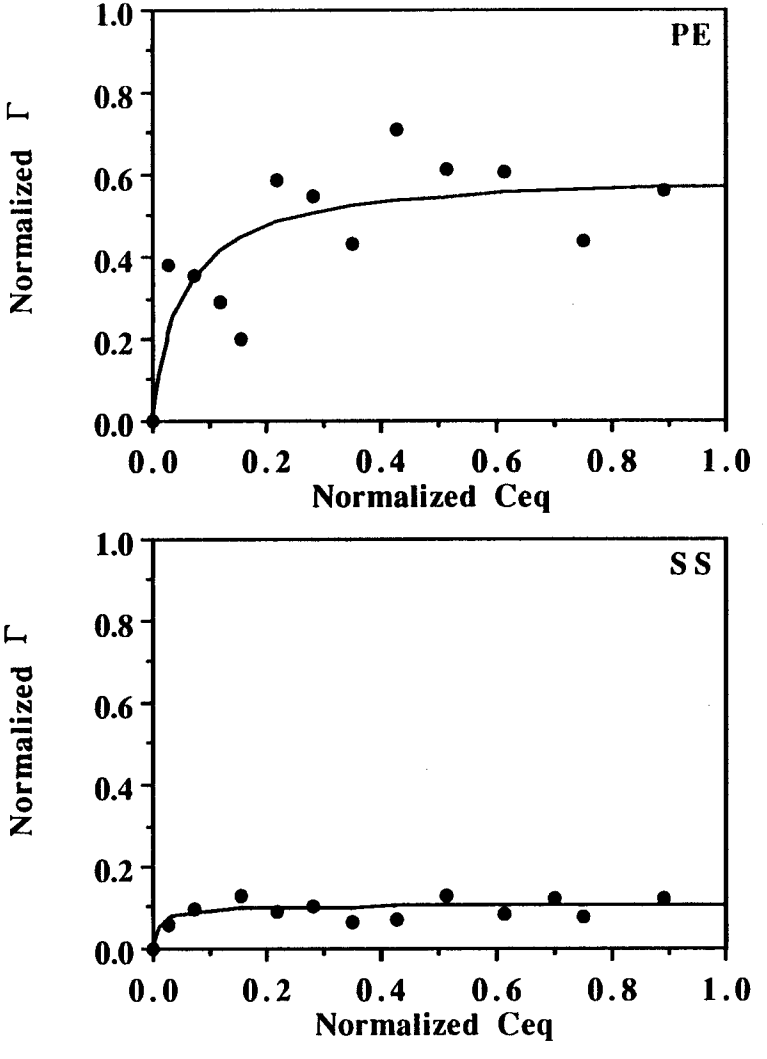

Figure 4.2 (continued)

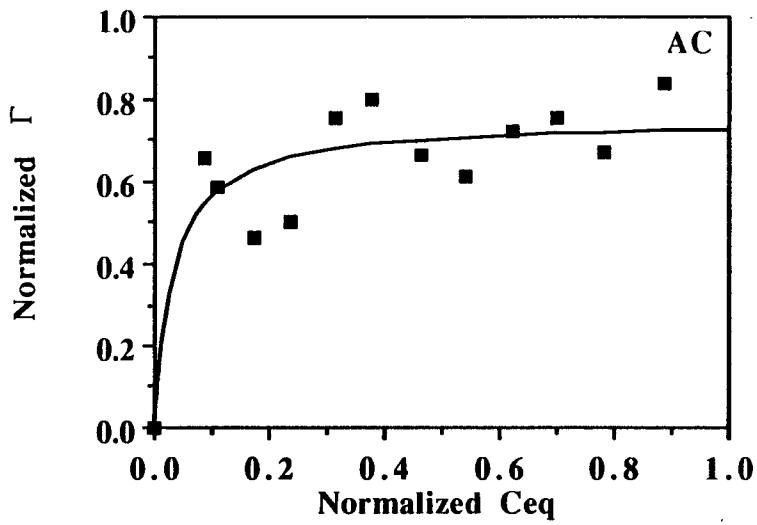

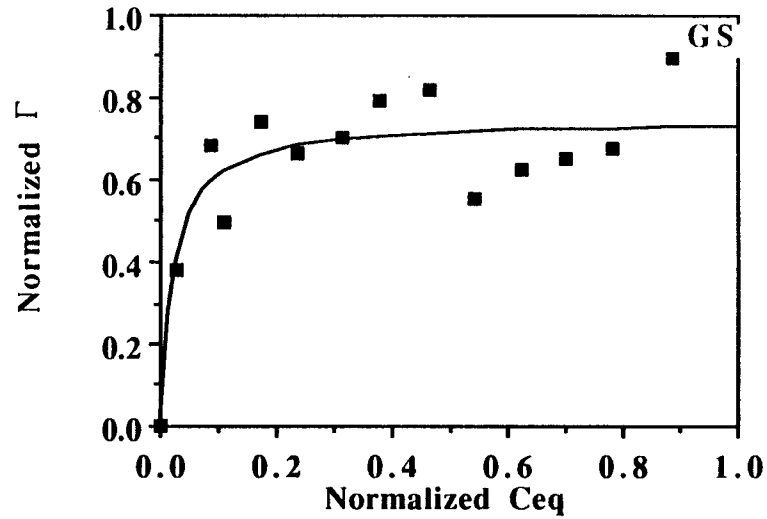

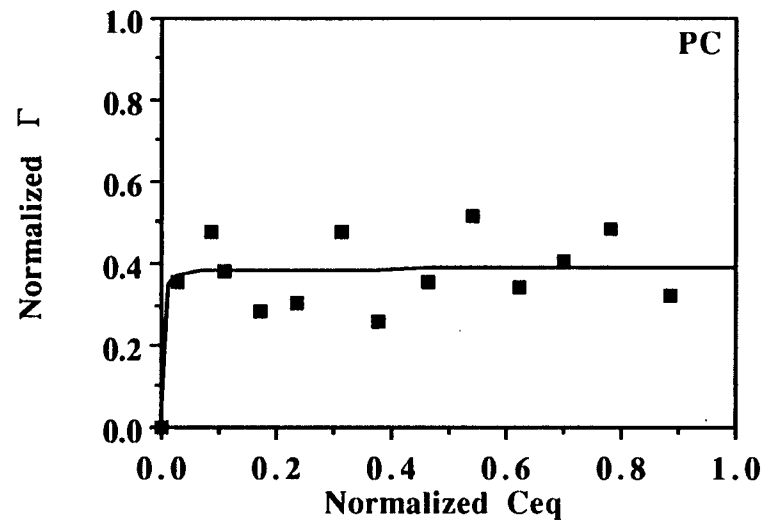

Figure 4.3

Experimentally measured adsorption data fit to the Langmuir-type isotherm for each material at 55°C.

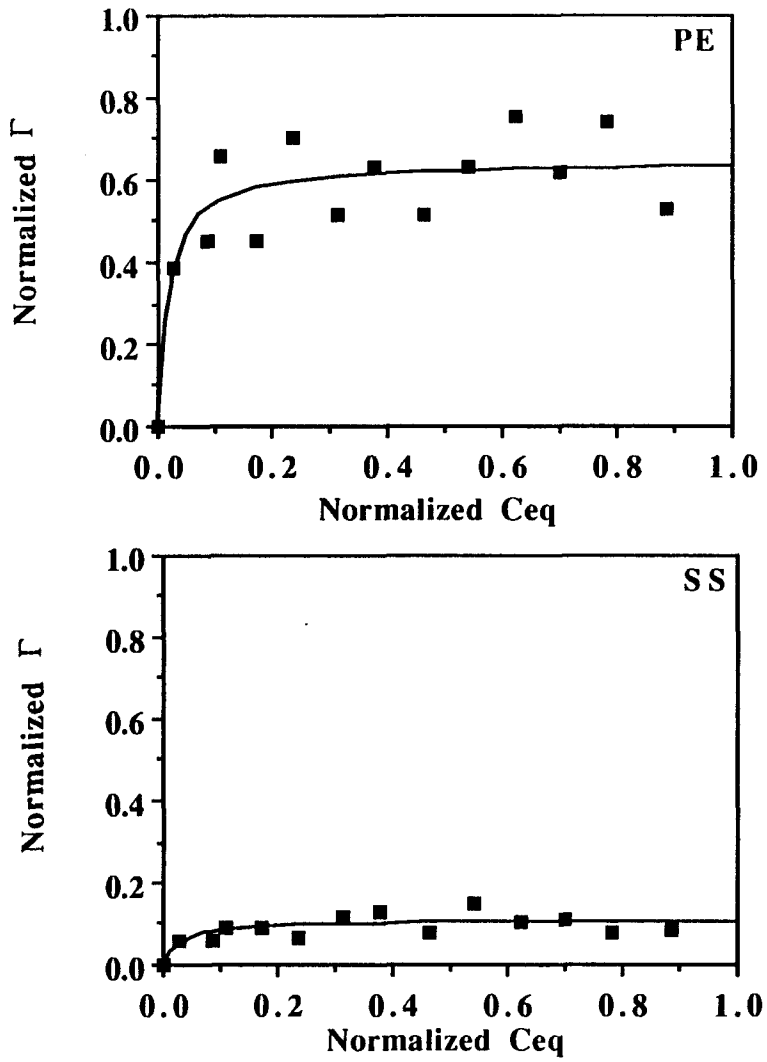

Figure 4.3 (continued)

Table 4.1 The parameters of the Langmuir-type model (equation 3.10) (their associated standard errors shown in parentheses), used to describe β-lactoglobulin adsorption on each surface at each temperature [$\Gamma = \Gamma_{max}\ C_{eq} / (b + C_{eq})$].

Material	**Temperature**	Γ_{max} [μg/cm^2]	**b [mg/l]**
Acrylic	25°C	2.63 (0.30)	3.1 (20.3)
Glass	25°C	2.99 (0.23)	35.3 (25.5)
Polycarbonate	25°C	2.35 (0.14)	103.6 (28.3)
Polyester	25°C	2.38 (0.22)	20.5 (22.0)
#304 SS	25°C	0.39 (0.04)	36.6 (35.1)
	***	*** *** ***	
Acrylic	37°C	2.45 (0.21)	37.2 (44.7)
Glass	37°C	2.60 (0.17)	77.1 (60.5)
Polycarbonate	37°C	1.96 (0.27)	230.2 (187.7)
Polyester	37°C	2.39 (0.31)	210.2 (144.4)
#304 SS	37°C	0.41 (0.04)	53.1 (55.7)
	***	*** *** ***	
Acrylic	55°C	2.99 (0.22)	131.9 (83.0)
Glass	55°C	2.98 (0.17)	87.8 (44.5)
Polycarbonate	55°C	1.54 (0.11)	5.2 (26.8)
Polyester	55°C	2.57 (0.15)	75.9 (43.6)
#304 SS	55°C	0.43 (0.04)	135.9 (97.0)

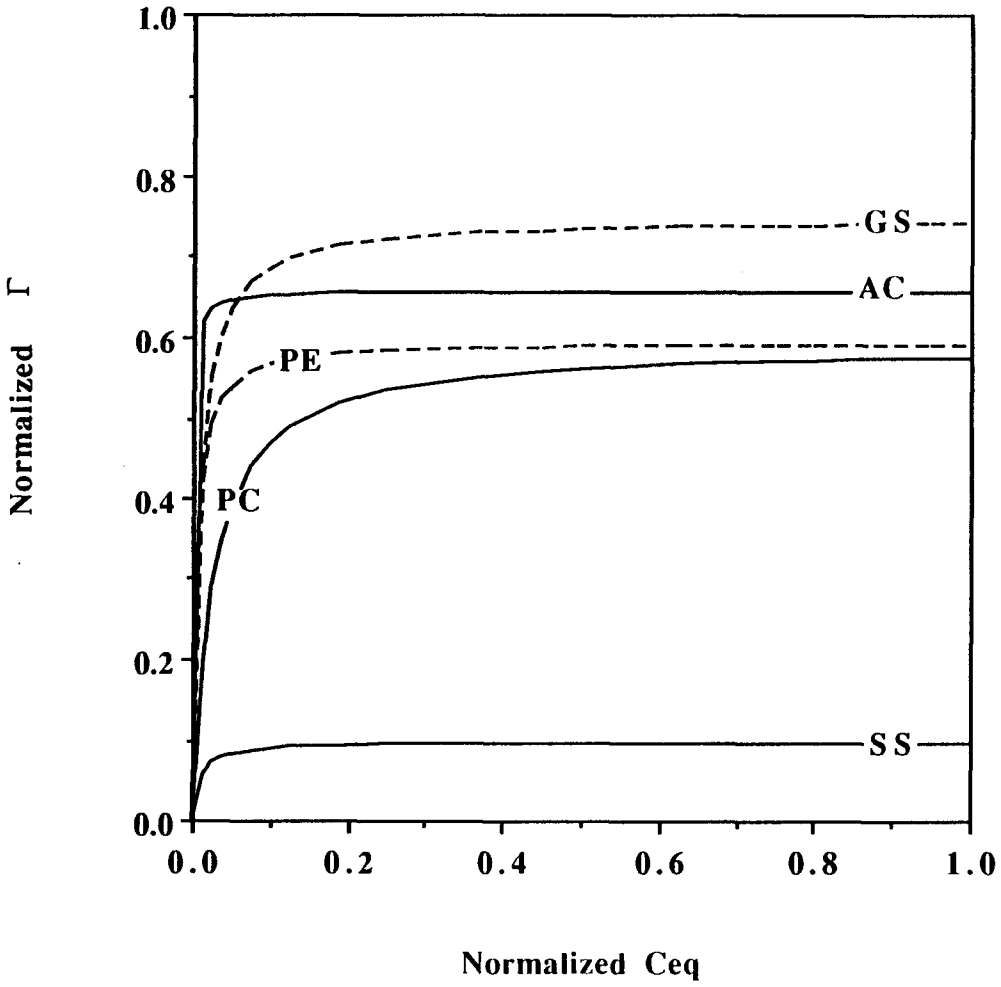

Figure 4.4

Comparison of the adsorption isotherms constructed for each material at 25°C.

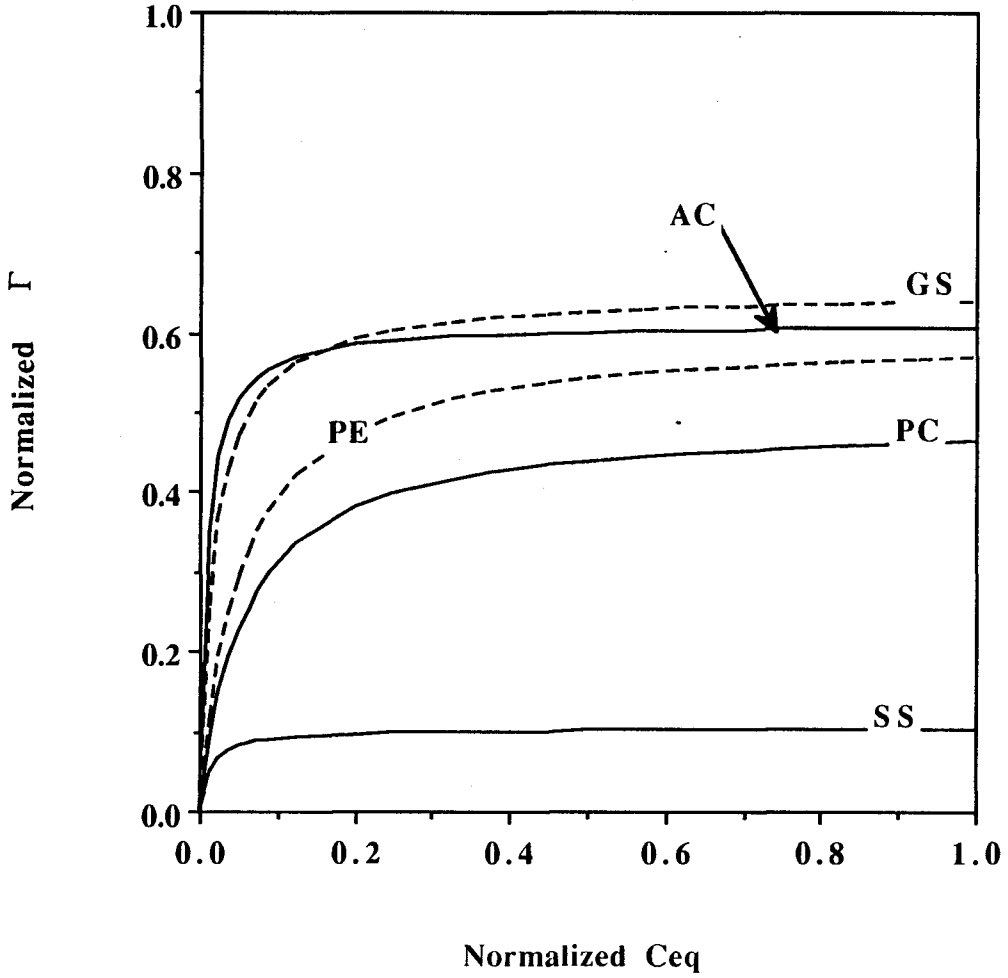

Figure 4.5

Comparison of the adsorption isotherms constructed for each material at 37°C.

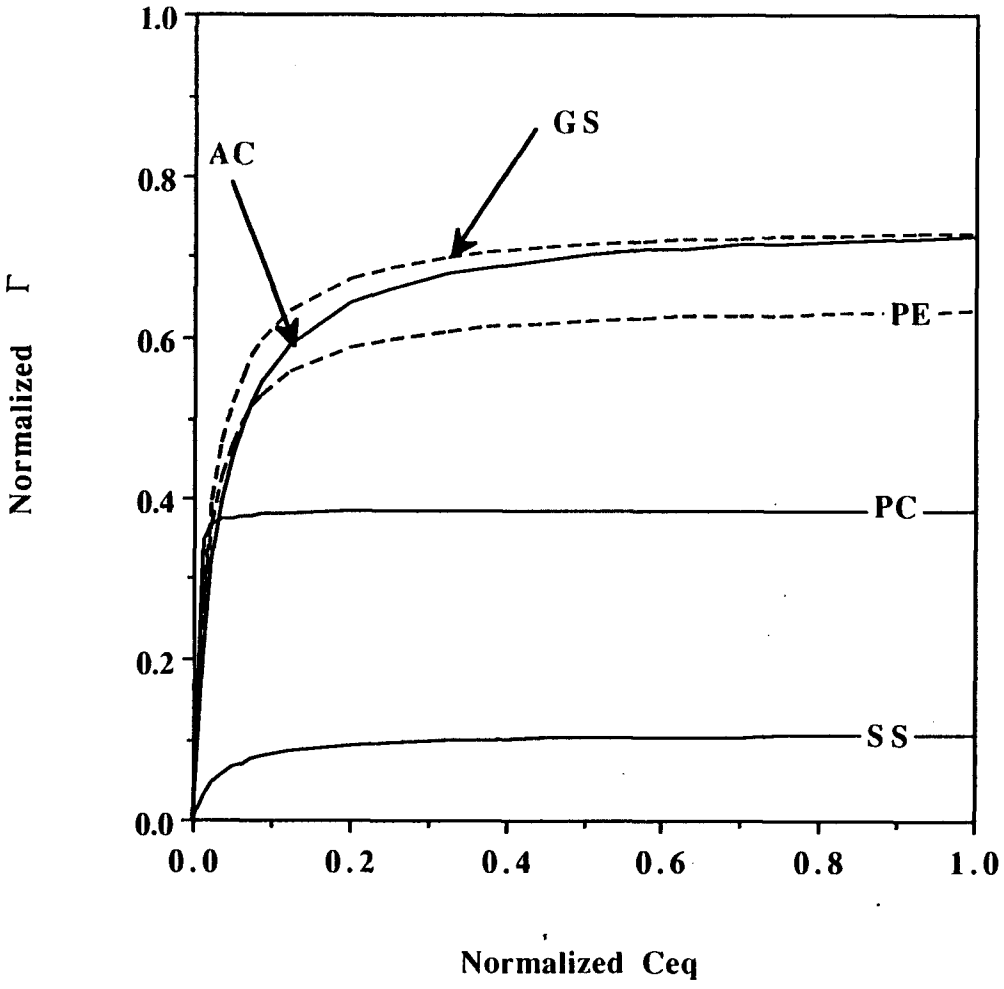

Figure 4.6

Comparison of the adsorption isotherms constructed for each material at 55°C.

A plot of the polar component of the work of adhesion, W_a^p [mJ/m^2], calculated from equation (3.4) versus the polar component of diagnostic liquid surface tension, γ_L^p [mJ/m^2], is shown in Figure 4.7. With the assumption that W_a^p is linearly dependent on γ_L^p, the slope, k, intercept, b, and their standard errors were recorded and are given in Table 4.2. In general, a surface characterized by a high slope, k, is more hydrophilic than that characterized by a low slope. Also shown in Table 4.2 is $W_a{}^p{}_{water}$ for each surface as calculated from equation (3.6).

As Lee and Ruckenstein indicated (11), a Hamaker constant, $A_{ps(w)}$ [J] can be defined, providing a quantitative indication of the strength of interaction between a protein molecule and a solid located in water:

$$A_{ps(w)} = -16\ \pi\ d_o^2\ \Delta F_{ps(w)}(d_o) \qquad (4.1)$$

where d_o is the equilibrium distance between protein and surface (approximately equal to 1.6×10^{-10} m); and $\Delta F_{ps(w)}(d_o)$ is the change in free energy [J/m^2] when protein and solid located in water are brought from infinite to equilibrium distance:

$$\Delta F_{ps(w)}(d_o) = \gamma_{sp} - \gamma_{pw} - \gamma_{sw} \qquad (4.2)$$

where

$$\gamma_{sp} = \gamma_s + \gamma_p - 2\ (\gamma_s^d\ \gamma_p^d)^{1/2} - 2\ (\gamma_s^p\ \gamma_p^p)^{1/2} \qquad (4.3)$$

$$\gamma_{pw} = \gamma_p + \gamma_w - 2\ (\gamma_p^d\ \gamma_w^d)^{1/2} - 2\ (\gamma_p^p\ \gamma_w^p)^{1/2} \qquad (4.4)$$

and

$$\gamma_{sw} = \gamma_s + \gamma_w - 2\ (\gamma_s^d\ \gamma_w^d)^{1/2} - 2\ (\gamma_s^p\ \gamma_w^p)^{1/2} \qquad (4.5)$$

All γ_i [J/m^2] refer to surface or interfacial energies, where the subscript: p stands for protein, s for solid, and w for water. As done by Lee and Ruckenstein (11), γ_s, γ_s^d, and γ_s^p were calculated according

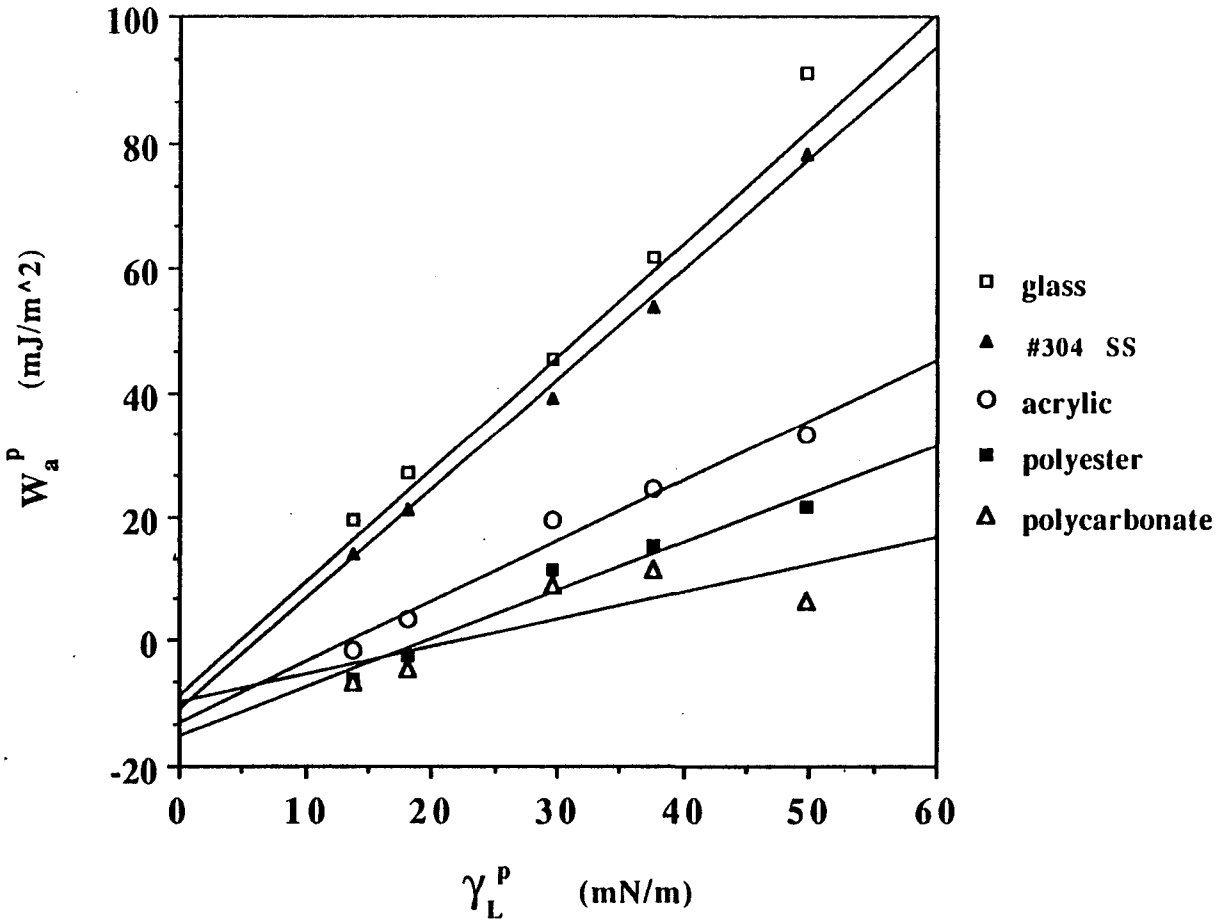

Figure 4.7 The relationship between the polar components of the work of adhesion and diagnostic liquid surface tension for each surface studied.

Table 4.2 Solid surface properties related to the hydrophobic-hydrophilic balance of each. ($W_a^P = k\ \gamma_L^P + b$). (the standard errors for k and b are shown in parentheses)

	$W_a^P{}_{water}$	k	b
Glass	87.94	1.95 (0.11)	-9.0 (3.6)
#304 SS	76.47	1.77 (0.06)	-11.4 (2.1)
Acrylic	35.19	0.98 (0.09)	-13.3 (2.9)
Polyester	23.49	0.78 (0.09)	-15.4 (2.9)
Polycarbonate	11.99	0.44 (0.20)	-10.1 (6.5)

to Kaelble (17). Surface properties of protein (i.e., γ_p, γ_p^d, and γ_p^p) were taken from Lee and Ruckenstein (1988) as well, with, $\gamma_p = \gamma_w$. For each solid surface, the Hamaker constant was evaluated using the set of equations (4.1) through (4.5); the results are shown in Table 4.3.

The temperature-dependence of β-lactoglobulin adsorption on each surface was observed to be more or less similar, with the exception of #304 SS. Polyester isotherms are shown in Figure 4.8, as an example of what was observed with the glass and polymers (except for polycarbonate). Isotherms constructed for #304 SS are shown in Figure 4.9.

Table 4.3 Estimated values of the Hamaker constant, $A_{ps(w)}$ [J]. (the standard error is 3.9×10^{-21} for each surface).

Surface	$A_{ps(w)}$
Glass	5.76×10^{-21}
#304 SS	10.34×10^{-21}
Acrylic	13.93×10^{-21}
Polyester	14.65×10^{-21}
Polycarbonate	15.56×10^{-21}

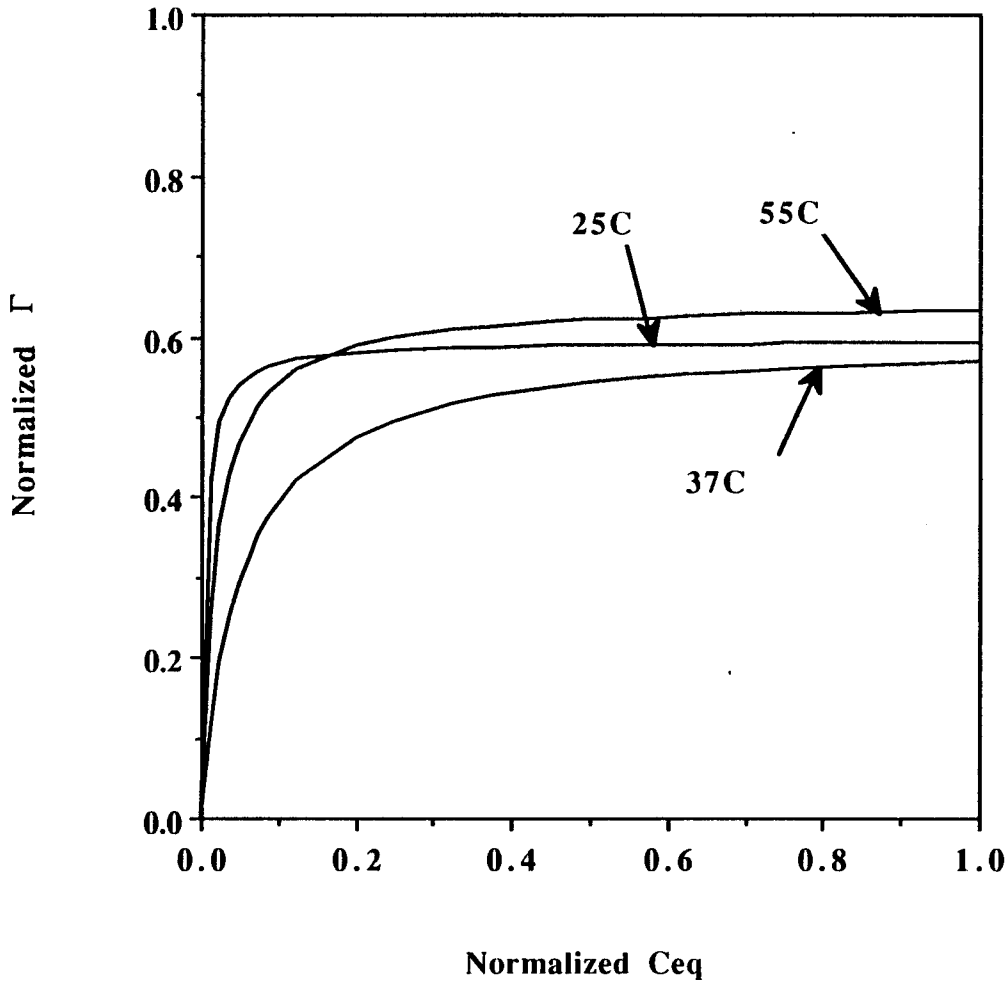

Figure 4.8

Adsorption isotherms constructed for polyester at 25, 37, and 55°C.

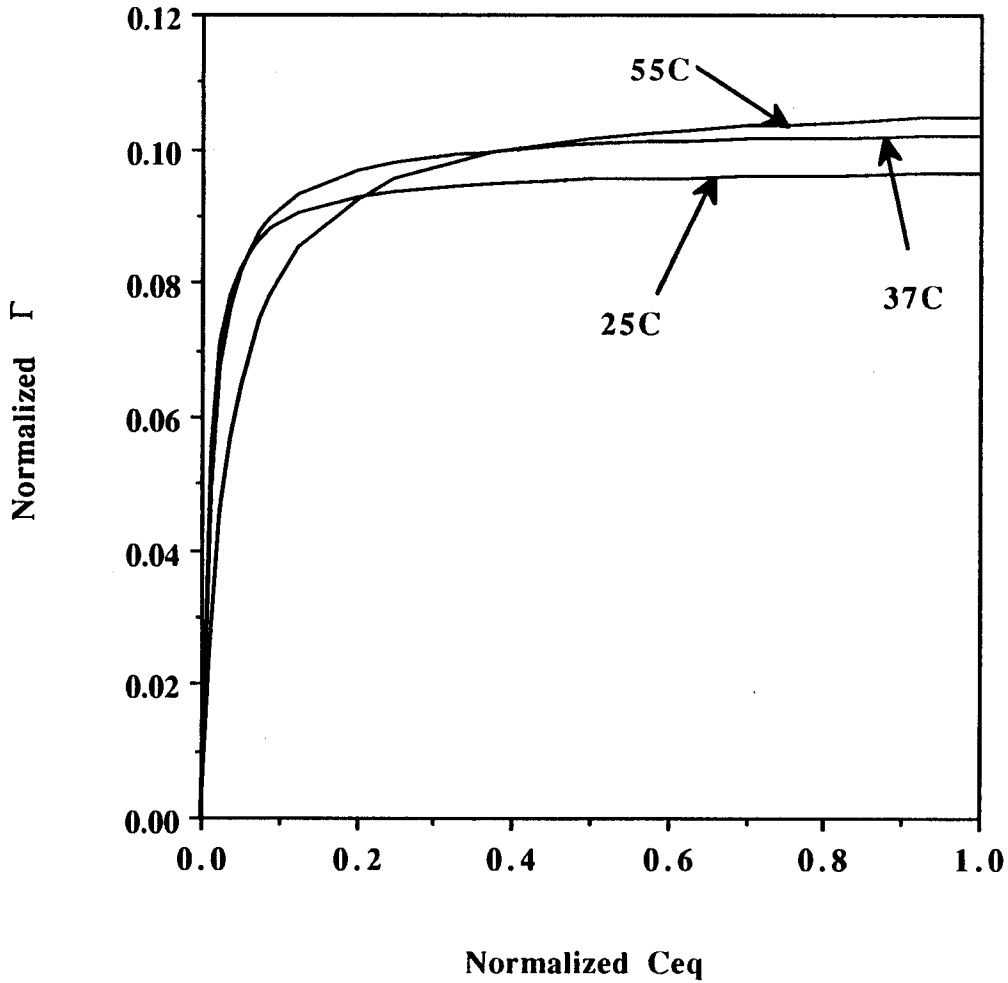

Figure 4.9

Adsorption isotherms constructed for #304 SS at 25, 37, and 55°C.

5. DISCUSSION

5.1 Applicability of the Langmuir-Type Model

A Langmuir-type equation was adopted to describe each β-lactoglobulin adsorption isotherm. Although it is known that the premises of the Langmuir model were not fulfilled, it best described the pattern of the experimental data, based purely on non-linear curve fitting. The pattern was such that the surface apparently saturated at low bulk concentration and adsorbed mass was observed to remain nearly constant beyond these low values of concentration. For each isotherm, Langmuir-type and Freundlich models were each used to describe the pattern of the experimental data; overall, the Langmuir-type model was found to fit better than the Freundlich model. The objective was to study relative rather than absolute adsorptive behavior as it is affected by temperature and surface properties; a model was employed purely for this purpose. Moreover, for this reason, normalization of both the apparent equilibrium concentration and the adsorbed mass of protein was chosen as a more appropriate method of presenting the data.

Table 4.1 indicates that the curve-fitted plateau value, Γ_{max}, should be regarded as a more reliable feature of the isotherm than the value of initial slope of the curve, where $C_{eq} \ll b$. This is probably due to the fact that it was difficult to accurately measure the adsorbed mass of protein at low surface concentrations. Also, application of ellipsometry to non-specular, anisotropic engineering materials is a challenge in itself, although other investigators have met the challenge

with success. For example, Engström and Bäckström (18) used ellipsometry as a tool to study detergency at hard surfaces. Using the Lorentz-Lorenz equation, they calculated the adsorbed mass of lipids formed on poly(vinyl chloride), a typical polymer, and chromium surfaces. Next, they compared the calculated, adsorbed mass to the mass obtained using a radiotracer technique. Their comparisons showed that the mass determined by ellipsometry deviated from radiotracer results by at most about +/- 10%.

Figures 4.1, 4.2, and 4.3 show the experimental data recorded at 25, 37, and 55°C, respectively. They also enable visualization of how effectively the Langmuir-type equation describes the pattern of data. Although adsorption isotherms constructed for the surfaces of acrylic, polyester, and to a lesser extent, glass, are characterized by a more pronounced degree of scatter, the Langmuir-type equation more or less fits the pattern of data recorded at each temperature.

5.2 Surface Effects

As seen in Figures 4.4, 4.5, and 4.6, the value of adsorbed mass of β-lactoglobulin was found to be greatest on glass, then on acrylic, polyester, polycarbonate, and #304 stainless steel in descending order. This relationship among materials, with respect to order, was essentially temperature-independent between 25 and 55°C. Although protein adsorption is hydrophobic in nature (i.e., entropically driven), solid surface hydrophobicity per se is certainly not the universally acknowledged criterion by which protein adsorption can be identified or

described. One should expect that there are other factors that can significantly contribute to the overall process of adsorption. Some of these factors include surface energetics, electrostatics, protein characteristics, and microenvironmental conditions.

The substrates under investigation included both polymeric and non-polymeric materials. Adsorption on each type of material will be interpreted separately. The reason to split them in this manner is that protein adsorption on polymers is unique and sometimes difficult to describe or predict. This diversity in behavior results from the surface anisotropy of polymers, which in turn emanates from various crystallographic or morphological orientations adopted at the surfaces, and from variations in the binding of an individual atom within the polymer structure at different points along its surface.

Adsorption on Polymers. Looking at Figure 4.7 and Table 4.2, one sees that among polymers, acrylic exhibits the most hydrophilic, and polycarbonate the least hydrophilic (i.e., most hydrophobic) surface. A Hamaker constant, which is a measure of the strength of interaction between a protein and a solid surface located in water, was calculated for each material and listed in Table 4.3. It was found that the polycarbonate surface has the largest value of Hamaker constant, whereas glass, the least hydrophobic surface, produced the smallest value of Hamaker constant. The Hamaker constant correlates with solid surface hydrophobicity; indeed, both seem to quantify the same property of a surface. Nevertheless, the acrylic surface adsorbed more protein than that of polycarbonate, which presents somewhat of a contradiction considering the hydrophobic nature of protein adsorption. Lee and

Ruckenstein (11) found a similar anomaly in a study of the adsorption of proteins onto polymeric surfaces of different hydrophilicities, i.e., the most hydrophobic material was found not to adsorb the greatest amount.

It appears likely that one or several other factors are involved in the overall process. For example, a comparison of the molecular structure of each polymer indicates (19) that acrylic is a soft, extensible material resulting from high molecular flexibility in addition to an amorphous, coiled structure. On the other hand, polycarbonate is a rigid, inextensible material, and to some degree is crystallizable (19). Polyester has physical properties that lie in between. The interaction between these polymer surfaces and water, as was observed from the contact angle measurements and shown in Figure 4.7, supports this classification based on molecular and morphological structure. Consider the drop of water formed on the acrylic surface. The experimental value of W_a^P was nearly equal to that obtained by the straight line equation, providing an indication that water had penetrated to some extent through the amorphous structure. However, with water on the polycarbonate surface, the situation was reversed. Therefore, in this case it is likely that adsorbed mass can be correlated somewhat to extensibility of the polymer structure. This correlation can be explained by the fact that an extensible structure, like an amorphous structure, provides more surface area for adsorption than a stiff structure. Moreover, an amorphous structure is more likely to undergo surface restructuring (i.e., relaxation) than is a crystallizable structure. In other words, an amorphous structure

affords more capability than a crystallizable structure to accommodate an adsorbate.

Adsorption on Non-Polymeric Materials. Adsorption on such materials can at least be partially explained in terms of surface energetics. In agreement with studies of Absolom et al. (20) and Baier (21) in which cell adhesion was correlated to surface energetics, glass (a high-energy surface) was observed to adsorb the greatest mass of β-lactoglobulin. Stainless steel, certainly a high-energy surface relative to polymer surfaces, did not adsorb to the extent expected for a typical high-energy surface. Nevertheless, plateau values of protein adsorption on stainless steel were found to be consistent with those reported elsewhere (22,23), and lie within the range of adsorbed mass on metal surfaces in general (24,25,26). Moreover, unlike the transparent glass and polymers, stainless steel fits under a separate catageory of materials from an ellipsometric standpoint. It may consequently be inappropriate to compare results obtained on stainless steel with those obtained on the transparent materials.

5.3 Temperature Effect

The temperature dependence of β-lactoglobulin adsorption could not be clearly identified for several reasons. Although protein adsorption is expected to increase with increasing temperature due to increased strength of hydrophobic bonding as well as decreased protein stability in solution, some investigators (5,13) consider the temperature effect on adsorption to be absent or very small. In any event, one might

expect that the plateau value exhibited by isotherms should be greatest at 55°C, lowest at 25°C, with that at 37°C falling somewhere in between. However, Figure 4.8 shows that for polyester, taken as representative of all transparent materials, with the exception of polycarbonate, this order with respect to 25°C and 37°C was reversed. Figure 4.9, constructed for stainless steel, shows that the expected order of isotherms was preserved. The plateau value recorded for each surface at 55°C was found to be greatest on all substrates except polycarbonate. Since the temperature effect may be very small, and since some of the data exhibit a relatively large degree of scatter, the temperature dependence of β-lactoglobulin adsorption is difficult to quantify at best, especially with respect to polymers. Arnebrant et al. (13) studied the temperature dependence of adsorption for α-lactalbumin and β-lactoglobulin on chromium surfaces. They observed that the curves for β-lactoglobulin at 25, 66, 70, and 73°C were rather similar. It was only when the temperature exceeded the denaturation temperature (79°C) of β-lactoglobulin, that they could observe a significant difference in the adsorbed mass.

It should also be noted that in this work on the average, the total number of data points taken at 25°C was equal to ten per surface, whereas the number at both 37°C and 55°C was equal to thirty. Consequently, the 25°C isotherms may be less reliable than isotherms at either of the other temperatures. As a consequence, the plateau values recorded on transparent materials at 25°C, which appeared to be greater than the plateau values recorded from the 37°C-isotherms, are suspect.

5.4 Monolayer Versus Multilayer Film

Finally, comparing the plateau values of the isotherms to that for a β-lactoglobulin monolayer (0.1 $\mu g/cm^2$ side-on configuration, 0.5 $\mu g/cm^2$ close-packed configuration), indicates that adsorption on stainless steel lies within the range of monolayer adsorption; whereas, adsorption on glass and polymers exhibited multilayer film formation. The classification of protein adsorption, in general, into monolayer adsorption or multilayer film formation is basically theoretical rather than experimentally verified. It is merely based on the magnitude of adsorbed mass and/or on the film thickness with respect to protein dimensions in solution (9,10,27).

6. CONCLUSIONS

1. β-Lactoglobulin adsorption satisfactorily fits a Langmuir-type model, where a steep initial slope over very low protein concentration is followed by attainment of a plateau value at higher concentration.
2. Although protein adsorption is entropically driven, solid surface hydrophobicity does not completely explain the pattern of the data.
3. For polymers, protein adsorption can be explained with reference to molecular extensibility (or degree of amorphous character). An amorphous structure is more likely to undergo surface restructuring than is a crystallizable structure, thus affording a greater capability to accommodate an adsorbate.
4. Ellipsometry works well with specular surfaces of high substrate refractive index. However, with less specular surfaces (e.g. polymers) the experimental data exhibit a pronounced degree of scatter.
5. Temperature effects on the adsorption of β-lactoglobulin appears to be insignificant.

7. RECOMMENDATIONS

1. For a better understanding of the effects of both solid surface properties and molecular properties on adsorption, use of specular surfaces exhibiting relatively high substrate refractive indices is recommended.
2. For a better understanding of the temperature effect on protein adsorption, expanding the temperature range above the denaturation temperature is helpful.
3. To study protein adsorption at very low concentrations (i.e., less than 100 mg/l), application of another technique (e.g. radiolabelling and IR-spectroscopy) is suggested.
4. With engineering materials (i.e., less specular surfaces), use of some technique in parallel with ellipsometry is suggested to better quantify protein adsorption and at the same time serve to calibrate the ellipsometer.

REFERENCES

1. Stryer, L. (1988). *Biochemistry*, W.H. Freeman and Company, New York.
2. Fasman, G.D. (1989). *Prediction of Protein Structure and the Principles of Protein Conformation*, Plenum Press, New York and London.
3. Andrade, J.D. (1985). *Surface and Interfacial aspects of Biomedical Polymers*, **2**, Plenum Press, New York and London.
4. Slejko, F.L. (1985). *Adsorption Technology: A step-by-Step Approach to Process Evaluation and Application*, pp. 1-6, Marcel Dekker, Inc., New York and Basel.
5. Parfitt, G.D. and C.H. Rochester (1983). *Adsorption from Solution at the Solid/Liquid Interface*, pp. 153-218, Academic Press, London.
6. De Feijter, J.A., J. Benjamins and M. Tamboer (1987). *Colloid and Surfaces*, **27**, pp. 243-266.
7. Levine, S.N. (1969). *J. Biomed. Mater. Res.*, **3**, pp. 83-94.
8. Horbett, T.A., "The Kinetics of Adsorption of Plasma Proteins to a Series of Hydrophilic-Hydrophobic Copolymers", in: *Adhesion and Adsorption of Polymers*, (Lee, Lieng-Huang, ed.), **2**, pp. 677-682, (1980), Plenum Press, New York and London.
9. De Feijter, J.A., J. Benjamins, and F.A. Veer (1978). *Biopolymers*, **17**, pp. 1759-1772, John Wiley & Sons, Inc.
10. Brash, J.L. and D.J. Lyman (1969). *J. Biomed. Mater. Res.*, **3**, pp. 175-189.

11. Lee, S.H. and E. Ruckenstein (1988). *J. of Colloid and Interface Science*, **125**, No. 2, pp. 365-379.

12. Baier, R.E. (1969). *J. Biomed. Mater. Res.*, **3**, pp. 191-206.

13. Arnebrant, T., K. Barton, and T. Nylander (1987). *J. of Colloid and Interface Science*, **119**, No. 2.

14. McGuire, J. and S.A. Kirtlty (1988). *J. of Food Engineering*, **8**, pp. 273-286.

15. McGuire, J. (1990). *J. of Food Engineering*, **12**, pp. 239-247.

16. Cuypers, P.A., J.W. Corsel, M.P. Janssen, J.M.M. Kop, W.T. Hermens, and H.C. Hemkers (1983). *The J. of Biological Chemistry*, **258**, No. 4, pp. 2426-2431.

17. Kaelble, D.H. (1970). *J. of Adhesion*, **2**, pp. 66-81.

18. Engström, S. and K. Backström (1987). *Langmuir*, **3**, pp. 568-574.

19. Deanin, R.D. (1972). *Polymer Structure, Properties and Applications*, pp. 6, 125-181, and 439-451, Cahners Book, Pennsylvania, U.S.A.

20. Absolom, D.R., L.A. Hawthorn, and G. Chang (1988). *J. Biomed. Mater. Res.*, **22**, pp. 271-285.

21. Baier, R.E. (1970). Surface Properties Influencing Biological Adhesion, in: *Adhesion in Biological Systems*, (R.S. Manly, Ed.), Academic Press, N.Y.

22. Enckevort, H.J.V., D.V. Dass, and A.G. Langdon (1984). *J. of Colloid and Interface Science*, **98**, No. 1.

23. Kim, J.C. and D.B. Lund, "Adsorption of β-Lactoglobulin onto Stainless Steel Surfaces", in: *Fouling and Cleaning in Food Processing*, (Heinz G. Kessler and Daryl B. Lund, ed.), pp.

187-199, (1989), Druckerei Walch, Augsburg, Federal Republic of Germany.

24. Elwing, H. and C.G. Gölander (1990). *Adv. in Colloid and Interface Science*, **32**, No. 2., pp. 317-339.

25. Wahlgren, M. and T. Arnebrant (1990). *J. of Colloid and Interface Science*, **136**, No. 1., pp. 259-265.

26. Arnebrant, T. and T. Nylander (1986). *J. of Colloid and Interface Science*, **111**, No. 2., pp. 529-533.

27. MacRitchie F. (1972). *J. of Colloid and Interface*, **38**, No. 2, pp. 484-488.

28. Creighton, T.E. (1983). *Biopolymers*, **22**, pp. 49-58.

29. Sauer R.T., K. Hehir, R. Stearman, M.A. Weiss, A. Jeitler-Nilsson, E.G. Suchanek, and C.O. Pabo (1986). *Biochemistry*, **25**, pp. 5992-5998.

30. Fersht, A.R. (1987). *Trends Biochem. Sci.*, **12**, pp. 301-304.

31. Fersht, A.R., J.P. Shi, J. Knill-Jones, D.M. Lowe, A.J. Wilkinson, D.M. Blow, P. Brick, P. Carter, M.M.Y. Waye, and G. Winter (1985). *Nature*, **314**, pp. 235-238.

32. Klapper, M.H. (1971). *Biochim. Biophys. Acta*, **229**, pp. 557-566.

33. Chothia, C. (1975). *Nature*, **254**, pp. 304-308.

34. Thornton, J.M. (1982). *Nature*, **295**, pp. 13-14.

35. Barlow, D.J. and J.M. Thornton (1983). *J. Mol. Biol.*, **168**, pp. 867-885.

36. Becktel, W.J. and J.A. Schellman (1987). *Biopolymers*, **26**, pp. 1859-1877.

37. Warshel, A. (1987). *Nature*, **330**, pp. 15-16.

38. Privalov, P.L. and N.N. Khechinashvili (1974). *J. Mol. Biol.*, **86**, pp. 665-684.

39. Privalov, P.L., Yu. V. Griko, S. Yu. Venyaminov, and V.P. Kutyshenko (1986). *J. Mol. Biol.*, **190**, pp. 487-498.

40. Roe, R.J., "Selective Adsorption of Polymers from Solution", in: *Adhesion and Adsorption of Polymers*, (Lee, Lieng-Huang, ed.), **2**, pp. 629-641, (1980), Plenum Press, New York and London.

41. Takahashi, A., M. Kawaguchi and T. Kato, "Adsorption of Polyelectrolyte Studied By Ellipsometry", in: *Adhesion and Adsorption of Polymers*, (Lee, Lieng-Huang, ed.), **2**, pp. 729-749, (1980), Plenum Press, New York and London.

42. Lee, R.G. and S.W. Kim (1974). *J. Biomed. Mater. Res.*, **8**, pp. 251-259.

A P P E N D I C E S

APPENDIX A

PROTEINS AS MACROMOLECULES

A.1 PROTEIN CHEMISTRY

Proteins are biological macromolecules synthesized in cells for specific functions. They are high molecular weight polyamides. The monomeric building block of proteins is the α-amino acid, the general structure of which is:

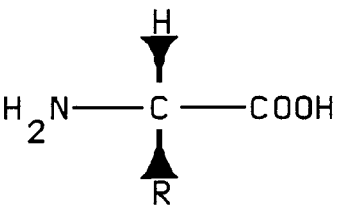

Thus, proteins are polymers formed by condensation of up to 20 different naturally occuring amino acids, differentiated according to the R group attached to the α-carbon atom. The condensation reaction occurs between the amino group of one amino acid and the carboxyl group of another, forming a peptide bond:

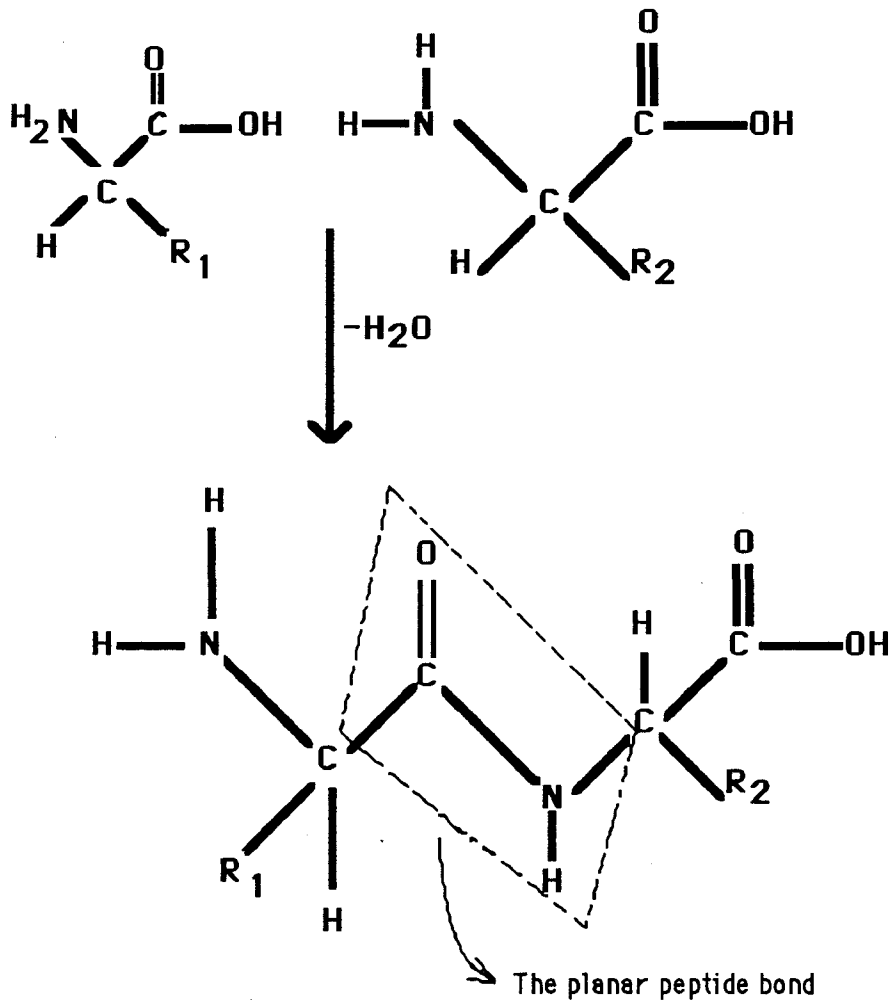

Such a giant macromolecule exists in an exquisitely complex structure. The words of Kendrew et al. (2), who managed to obtain the first high-resolution X-ray crystal structure of a protein are worth mentioning here: "Perhaps the most remarkable features of the molecule are its complexity and lack of symmetry. The arrangement seems to be almost totally lacking in the kind of regularities which one instinctively anticipates."

This complexity in protein structure is characterized by different levels: primary, secondary, tertiary, and quaternary structure. Primary

structure is described (1) by the amino acid sequence itself and the location of disulfide bonds (i.e., covalent connections within the protein molecule). Secondary structure describes the spatial arrangement of amino acid residues that are near one another in the linear sequence. An α-helix and β-sheet are typical examples of secondary structure. Tertiary structure defines the spatial arrangement of amino acid residues that are far apart in the linear sequence. If a protein has two or more polypeptide chains, each with its exclusive primary, secondary, and tertiary structure, such chains can associate to form a multi-chain quaternary structure. Hence, a quaternary structure refers to the spatial arrangement of such subunits and their interaction.

A.2 PROTEIN STABILITY

Protein molecules are stabilized by different intramolecular forces that play a key role in maintaining protein structure. In addition to the planar peptide bond that constitutes the backbone of the molecule, there are intramolecular forces, though smaller in magnitude than a covalent bond, that are as important as the peptide bond itself. These intramolecular interactions include disulfide linkages, hydrophobic bonding, hydrogen bonding, dispersion forces, and electrostatic forces.

A.2.1 THE DISULFIDE COVALENT BOND. These forces are thought (2) to stabilize proteins by reducing the conformational entropy of the unfolded chain. Statistical treatments have proposed that the destabilization of the unfolded state depends on the length of the loop

formed by a single cross link (2). From Creighton's work on protein stability (28), the stabilizing contribution of a disulfide bond (or other cross link) is determined by the size of the loop formed in the chain and by the compatibility of the cross link with the folded structure. Creighton (28) found that for a given loop size, the most effective cross link may be formed between groups that are rigidly held in an optimum orientation by the folded structure. Saur et al. (29) found that an intermolecular disulfide bond joining residue 88 in adjacent subunits of the protein λ repressor increases the melting temperature (T_m) of the N-terminal domain by approximately 10^0C.

A.2.2 HYDROPHOBIC FORCES. These forces are considered to be one of the most important contributions to protein stability. Hydrophobic interactions (3) are basically entropically driven interactions, largely due to order/disorder phenomena in the surrounding water. Water molecules order themselves at apolar interfaces, and this ordering is entropically undesirable. This driving force is accountable for the minimization of the surface area of air bubbles or oil droplets in water, hence, most of the hydrophobic amino acids are oriented towards the interior of the molecule.

Current estimates of amino acid hydrophobicity are based on the measured free energies of transferring side chains from water to organic solvents. The temperature dependence of the transfer of six liquid hydrocarbons to water was analyzed and the results were used to interpret thermodynamic data on the unfolding of hen lysozyme (2). For the unfolding of lysozyme, the temperature dependence of the associated changes in enthalpy (ΔH) and entropy (ΔS) could be largely accounted for

by the hydrophobic effect.

The temperature independent part of the associated enthalpy ΔH was large and favored folding, presumably because of non-covalent interactions in the folded state. The temperature independent part of the associated entropy (ΔS) was large and favored unfolding, presumably because of conformational entropy. From 10 to 100°C, the free energy of stabilization from the hydrophobic effect increased with temperature, and it reached a maximum at around 112°C assuming ΔCp is constant. This analysis suggested that cold denaturation is caused by weakening of the hydrophobic effect. Unfolding occurs at higher temperatures because the destabilizing contribution of the conformational entropy of the unfolded state ($T\Delta S_{conf}$) increases more rapidly with temperature than the stabilizing contribution of the hydrophobic effect.

A.2.3 HYDROGEN-BONDING. These forces are considered to be one of the major contributions to the largely temperature independent part of the enthalpy of stabilization. Due to their small size and electropositivity in covalent bonds, Hydrogen atoms are easily attached to electronegative atoms. Hydrogen bonds are very common in proteins and are partly responsible for the α-helix and β-sheet stabilities. Hydrogen bond partners are exchanged during folding. Intramolecular bonds are formed at the expense of intermolecular hydrogen bonds with water.

Studies of the dimerization of urea and δ-valerolactam in water led some investigators (2) to conclude that the heat of formation H-bonds may be -1.5 kcal/mole or more. Using aqueous N-methyl acetamide as a model for the peptide bond, they estimated that ΔH for H-bond

formation is close to zero. The latter result supported the view that as long as equal numbers of H-bonds are formed in the folded and in the unfolded state, H-bonds do not contribute to the difference between the free energies of the states. A central feature of this analysis is that H-bonds in the folded and unfolded states, are considered to be energetically equivalent. The concentration of donor and acceptor in water, around 110 M, is assumed to be the effective concentration of all H-bonding groups in both the folded and unfolded states.

Several authors (2) have indicated, however, that differences in the average geometry, the entropy of formation, and the average number of interacting partners can lead to significant energetic differences between H-bonds in the folded and unfolded states. To determine the range of potential contributions, the consequences of adding or removing specific H-bonding groups have been analyzed. Fersht (30) and Fersht et al. (31) studied protein-ligand complexes and nucleic acids, and concluded that H-bonds between uncharged donors and acceptors can contribute from 0.5 to 1.8 kcal/mole to the observed association energy. H-bonds between charged groups can contribute up to 6 kcal/mole.

A.2.4 DISPERSION FORCES. The importance of dispersion or van der Waals forces for protein stability hinges on differences in packing in the folded and unfolded states (2). Unfolding usually involves very small changes in the volume of the system, so the average interatomic distance remains constant. In other words, this implies that van der Waals forces do not change appreciably between the two states. However, the overall volume of the system is not an adequate measure of the sum of the interactions.

Klapper (32) and Chothia (33) found that, during folding, water is transferred to the relatively open bulk phase, and the atoms that form the protein interior become as densely packed as molecules in crystals of small organic molecules. This changes the neighbors of solvent and protein atoms (the unfolded chain is more hydrated), and it changes the distribution of interatomic distances. Both of these effects can alter van der Waals interactions.

A.2.5 ELECTROSTATIC FORCES. Proteins may be considered polyelectrolytes since ionizable groups from amino acid side chains (Asp, Glu, Tyr, Lys, His, Arg, and Cys) and from C and N terminal amino acids participate in the acid-base equilibrium. Ionizable groups are not distributed randomly over protein surfaces, reflecting their individual structural and functional roles.

Thornton (34) and Barlow and Thornton (35) found that including the peptide dipoles, charges are, on average, surrounded by charges of the opposite sign. On average, only a third of the charged residues in proteins are involved in ion pairs, and 76% of these are between residues in different elements of secondary structure, and 17% of the ion pairs are buried, and these generally play clearly identifiable functional roles.

Overall, however, ion pairs are poorly conserved in protein families, suggesting that some of them are not critical for folding and stability. Becktel and Schellman (36) suggested that interactions of ionizable groups vary with pH, and the stability of a protein depends on the number of protons bound or released on denaturation. For many proteins, stability varies smoothly with pH, suggesting a presence of

compensating interactions amongst the ionizable groups. The strength of ionic interactions can be affected by changes in local net dielectric constants. The local dielectric constants within a protein can be quite high because of the distribution of polar groups. Warshel (37) suggested that local differences in polarity have been assumed to contribute to the 2.7 kcal/mole difference in the stability of an Asp-Arg ion pair compared to the inverted Arg-Asp pair in aspartate amino transferase.

A.3 PROTEIN CONFIGURATION

Protein denaturation involves a conformational change. The total free energy change or the stabilization free energy between the folded (native) state and the unfolded (denatured) state varies from five to fifteen kcal/mole. This narrow range of stabilization is independent of molecular weight (2). Upon unfolding, the polypeptide chain becomes less compact and more highly solvated, and much more flexible. Of course, the unfolded polypeptide cannot be an ideal mathematically random chain. It has been shown (2) that excluded volume effects alone reduce the estimated number of allowed backbone conformations of a 100 residue chain from about 10^{60} in a "random" coil to about 10^{16}.

Protein denaturation is a highly cooperative reaction, and the protein stability depends on environmental conditions such as temperature, pressure, pH, ionic strength, and the concentration of specific ligands, stabilizers, and denaturants. A central feature of the energetics of protein denaturation is that changes in enthalpy and

entropy are strongly dependent on temperature. In particular (2):

$\Delta H_T = \Delta H_O + \Delta Cp\ (T-T_O)$

$\Delta S_T = \Delta S_O + \Delta Cp\ \ln(T/T_O)$

where ΔH_T and ΔS_T are the changes in enthalpy and entropy at temperature T, ΔH_O and ΔS_O are the changes in enthalpy and entropy at a reference temperature T_O, and ΔCp is the difference in heat capacity between the folded and unfolded states at constant pressure. ΔCp for unfolding is large and positive (1-2 kcal/mol-K). Moreover, it is also constant or nearly constant in the temperature range studied (38) (0 - 80°C).

This behavior has been taken as evidence for the central role of the hydrophobic effect in protein stabilization. The large value of ΔCp means that ΔH_T and ΔS_T are steep functions of temperature. A temperature change of 1°C causes changes in ΔH_T and in $T\Delta S_T$ of approximately 1-2 kcal/mole, and ΔH_T and ΔS_T are zero near room temperature. Given that $\Delta G_T = \Delta H_T - T\Delta S_T$, the free energy of stabilization reaches a maximum near room temperature, where $\Delta S_T = 0.0$, and the equilibrium constant for folding ([F]/[U]) reaches a maximum at a slightly lower temperature (36), where $\Delta H_T = 0.0$

At higher temperatures, unfolding results in a large increase in entropy, because of the added flexibility of the polypeptide chain, and a compensating increase in enthalpy, due to changes in interactions in the protein and solvent. At lower temperatures, the system loses entropy and releases heat on unfolding (39).

APPENDIX B

ADSORPTION

Adsorption involves migration of a substance from one phase to the surface of an adjacent phase, accompanied by its accumulation at the interface (4). The adsorbing phase is called the adsorbent, and the material concentrated at the interface is called the adsorbate. Adsorption is a result of the binding forces between individual atoms, ions or molecules of an adsorbate and the adsorbent surface. These binding forces or interactions vary in magnitude from the weak van der Waals type of binding (i.e., physical adsorption) to the strong covalent type of binding (i.e., chemisorption).

Polymer adsorption in general, and biopolymer adsorption in particular show a range of binding energies depending on the type of forces involved in adsorption. Polymer adsorption differs drastically from that of small molecules. This is basically due to the large number of conformations that a macromolecule can have, both in the bulk of a solution and at the interface. The entropy loss or gain associated with a given flexible polymer can be greater than that for small molecules or relatively stiff molecules (5).

Theoretical treatments of polymer adsorption are in essence statistical, for it is practically inconvenient if not impossible to account for all possible variations in configuration as a function of pertinent variables.

Although a comprehensive quantitative understanding of polymer adsorption has eluded theoreticians as well as experimentalists, some qualitative or semi-quantitative trends have been observed. Some important observations are mentioned below (5):

1. Many types of polymers adsorb from solution onto a variety of surfaces. Multiple segments (footholds) cling to the surface, and a minimum adsorption free energy per segment is required to sustain this attachment.
2. Polymer adsorption isotherms have a "high affinity" character, i.e., in the initial part of the isotherm, at very low concentrations, the adsorbed amount rises steeply, while at higher concentrations it reaches a plateau.
3. The influence of temperature is small or absent.
4. It can be difficult to desorb polymers by dilution, but they can be exchanged with low molecular weight solutes, or with similar sized solutes.
5. Polymer adsorption is a slower process than adsorption of low molecular weight substances, for they are expected to have smaller diffusion coefficients and may require more time to undergo conformational changes.
6. Adsorption increases with decreasing solvent quality.
7. Adsorption increases with molecular weight in a poor solvent, and is rather insensitive to molecular weight in a good solvent.

A "good" solvent is one whose Flory-Huggins interaction parameter, χ, has a value less than zero. A "poor" solvent has a χ value greater

than zero; a χ value of zero indicates an athermal solvent. The physical meaning of χ can be visualized by considering an exchange process in which a segment in pure bulk polymer is exchanged with a solvent molecule in pure solvent, thereby considering all non-covalent interaction energies. If the coordination number is denoted by z and the solvent is taken to be component 1, and the polymer component 2, then in the exchange process, z contacts of 1-1 type and z contacts of 2-2 type are broken, and 2z contacts of 1-2 type are formed. Thus, an exchange enthalpy of $z(2h_{12}-h_{11}-h_{22})$ is obtained, where h stands for the interaction enthalpy per contact. The parameter χ is expressed in terms of the net enthalpy change per solvent molecule i.e., for z contacts of the 1-2 type:

$$\chi = z\ (h_{12} - 1/2h_{11} - 1/2h_{22})\ /\ kT \qquad (B.1)$$

Thus, if $\chi<0$, the solvent is "good" since unlike contacts are preferred over like contacts. A similar parameter is used in polymer adsorption theories to account for the interaction of a segment with the surface. If there are z contacts that a segment or a solvent molecule on the surface can have with its neighbors and z′ of them are with the surface, then χ_S can be defined as follows:

$$\chi_s = z'(h_{s1} - h_{s2} + 1/2h_{22} - 1/2h_{11})\ /\ kT \qquad (B.2)$$

So if χ_S is positive, a polymer segment is preferred over a solvent molecule by the adsorbent. In principle, a minimum adsorption enthalpy is required for polymers to adsorb, which is equivalent to stating that there exists a critical χ_S value, χ_{SC}. It was shown[5] that this critical adsorption energy is of the order of a few tenths of kT per segment. It is worth mentioning here that theoretical models

used to predict polymer behavior at surfaces have employed both χ and χ_s, due to their composite properties to account for the entropic contributions of solvent orientation (i.e., hydrophobic interactions). The segment-surface interactions and conformational statistics of an adsorbed molecule were considered in detail by such models, and to a lesser extent so were the interactions of segments with each other.

Roe (40) discussed selective adsorption of polymers from solution. He considered two cases of solute polymers: the first case consists of solute polymers of the same chemical nature but of different chain lengths, and the second case consists of solute polymers of similar chain length but of different chemical identity. For the first case, he considered the free energy of the system as consisting of the summation, over the total number of segments, of the free energy per segment. Further, he expressed the free energy per segment as a function of the volume fractions of components in the system, the Flory-Huggins interaction parameter between the segments and that between the surface and segments, and the chain length.

The equilibrium composition profile was then obtained by minimizing the total free energy with respect to the volume fractions of the system to reach, after some mathematical manipulations, the following equation:

$$\phi^i_p/\phi^*_p = e^{\sigma r_p} \qquad \text{(B.3)}$$

where ϕ^i_p is the volume fraction (i.e., concentration) of component p at the interface, ϕ^*_p is the volume fraction of component p in the bulk solution, σ is a constant that depends on the composition of the system, and r_p is the chain length of component p. Equation (B.3) shows that

the ratio ϕ^i_p/ϕ^*_p increases with increasing chain length r_p. Consequently the adsorption of a high molecular weight species is preferred over one of lower molecular weight.

For the second case, where the chain length is similar among the components constituting the system, the ratio of surface fractions (concentrations) of components p and q, using the generalized form of the Langmuir adsorption isotherm for multisegment adsorption, was shown to be:

$$\theta_p / \theta_q = (K_p / K_q)\ (C_p / C_q) \qquad (B.4)$$

Consequently if the concentration of each species is the same, the adsorbance ratio θ_p/θ_q is equal to the ratio of the adsorption affinities K_p/K_q, which is the ν-th power of the ratio of the segmental adsorption affinities, where ν is the number of segments attached to the surface. This shows that, between two solute molecules of about the same chain length but of different chemical constitution, for a small difference in the adsorption affinity per segment an extreme preferential adsorption arises. In summary, Roe concluded that the total free energy change associated with the adsorption of polymer molecules arises mostly from the following three factors:

a. the change in the energy of interaction of the adsorbent surface with the solvent and solute molecules,

b. the change in the conformational entropy of the adsorbed polymers; and

c. the change in the entropy of mixing of the solute with the solvent.

Factor a is considered to be the major contributing factor to the total free energy in the case of chemically different solutes with the same chain length, and factor c is considered most important in the case of similar solutes with different chain length.

Takahashi (41) has studied the adsorption of polyelectrolytes using ellipsometry. He used sodium poly(acrylate) (MW = 950,000) dissolved in a NaBr solution. Platinum foils were used as the adsorbent. He found that the adsorbed amount attained a constant value within a few hours and remained unchanged for five days or more. For this particular case, he found that the adsorbed amount decreased with decreasing of ionic strength.

Based on his observations of film refractive index, thickness, and adsorbed mass, he suggested that electrostatic repulsion between charged groups on the polyions is responsible for the low adsorbed amount as well as the observed extension of the polyelectrolyte normal to the surface. By increasing the ionic strength, both intra- and inter-polyion interactions are weakened, and a higher adsorbed mass and lower degree of extension result. At very low polyelectrolyte concentrations, both the thickness and the adsorbed amount are low suggesting flattened conformation with a large number of attached segments at the surface predominating over other possible conformations. Further increase in polyion concentration results in the desorption of these segments, thus allowing more sites for further adsorption yielding a thicker adsorbed layer.

APPENDIX C

PROTEIN ADSORPTION

Surveying the literature, one can recognize that protein behavior at interfaces is a controversial issue. Keeping this in mind, the pertinent literature will be reviewed based on the author's opinion and on his own conclusions and suggestions.

C.1 THEORETICAL MODELING

A thermodynamic approach proposed by De Feijter et al. (6) for nonionic, flexible polymers is presented here, although protein is considered to be a somewhat rigid structure with some net charge. Their approach relies on a pseudo-lattice model (quasi-crystalline model), the cells of which may accommodate a solvent molecule (o), a polymer segment (p) or a surfactant molecule (s). Each macromolecule is thought to consist of m identical segments of which a fraction f is adsorbed directly to the surface, therefore $\nu = f.m$ cells of the surface layer are occupied by one adsorbed polymer. The volume fraction of the polymer in the bulk solution is ϕ_p, that of the surfactant ϕ_s, and that of the solvent $\phi_o = 1-(\phi_p+\phi_s) = 1-\phi$. At the surface, the polymer occupies a fraction θ_p of the surface cells, the surfactant occupies a fraction θ_s, and the solvent occupies the rest $\theta_o=1-(\theta_p+\theta_s)=1-\theta$. The rate of adsorption of a surfactant is proportional to its concentration (i.e., ϕ_s) in the bulk phase. It is also proportional to the

probability that the surfactant molecule finds a surface cell available for exchange, which in turn is proportional to the surface fraction $(1-\theta)$ occupied by solvent molecules. Therefore, the rate of adsorption of surfactant can be expressed as:

$$r_{s,ads} = k_1 \phi_s (1-\theta) \tag{C.1}$$

Similarly, the rate of surfactant desorption can be defined as

$$r_{s,des} = k_2 \theta_s (1-\phi) \tag{C.2}$$

At equilibrium, the rate of adsorption is equal to that of desorption; thus:

$$k_1 \phi_s (1-\theta) = k_2 \theta_s (1-\phi)$$

or:

$$\theta_s = K_s \frac{(1-\theta)}{(1-\phi)} \phi_s \tag{C.3}$$

where $K_s = k_1/k_2$.

For the polymer, the rate of adsorption is proportional to its concentration in the bulk solution and to the availability of surface cells for adsorption. For instance, the probability that a polymer finds one cell, occupied by a solvent molecule, is proportional to $(1-\theta)$, the probability that it finds two cells to $(1-\theta)^2$, and since ν segments of the polymer are involved in adsorption:

$$r_{p,ads} = k_3 \phi_p (1-\theta)^{\nu} \tag{C.4}$$

In a similar fashion, the rate of desorption of polymer will be:

$$r_{p,des} = k_4 \theta_p (1-\phi)^{\nu} \tag{C.5}$$

At equilibrium, both rates are equal, solving for θ_p yields:

$$\theta_p = K_p \frac{(1-\theta)^{\nu}}{(1-\phi)^{\nu}} \phi_p \tag{C.6}$$

where $K_p = k_3/k_4$.

From equations (C.3) and (C.6), the total surface fraction occupied by both the polymer and surfactant can be expressed in the form:

$$\theta = \theta_p + \theta_s = K_p \frac{(1-\theta)^{\nu}}{(1-\phi)^{\nu}} \phi_p + K_s \frac{(1-\theta)}{(1-\phi)} \phi_s \qquad (C.7)$$

The equilibrium constants K_p and K_s are functions of the adsorption energy of the protein and surfactant, respectively:

$$K_p = \exp(-\Delta E_p/kT) \qquad (C.8)$$

$$K_s = \exp(-\Delta E_s/kT) \qquad (C.9)$$

where $\Delta E_p = \nu \Delta e_p$ is the adsorption energy per polymer, Δe_p is the adsorption energy per polymer segment, ΔE_s is the adsorption energy of a surfactant, k is the Boltzmann constant, and T is the absolute temperature. The adsorption energies ΔE_p and ΔE_s are the energy changes associated with the transfer of a polymer or a surfactant from the bulk solution to the surface, and they have negative values when the species are surface active. For an athermal solvent case (Flory-Huggins interaction parameter, $\chi = 0.0$), ΔE_p and ΔE_s will be constant and independent of system composition.

If the system contains only a surfactant (i.e., $\theta_p = \phi_p = 0.0$) equation (C.3) will reduce to:

$$\theta_s / (1-\theta_s) = K_s \phi_s / (1-\phi_s) \qquad (C.10)$$

and for very low bulk concentration (i.e., $\phi_s << 1$), equation (C.10) becomes:

$$\theta_s / (1-\theta_s) = K_s \phi_s$$

or:

$$\theta_s = \frac{K_s \phi_s}{1 + K_s \phi_s} \qquad (C.11)$$

Equation (C.11) represents the well-known simple Langmuir isotherm. However, if the system contains only a polymer (i.e., $\theta_s = \phi_s = 0.0$), equation (C.6) will reduce to:

$$\theta_p \; / \; (1 - \theta_p)^{\nu} = k_p \; \phi_p \; / \; (1 - \phi_p)^{\nu} \qquad (C.12)$$

The last equation shows that protein adsorption, in general, need not to obey or follow Langmuir model which is described in terms of equation (C.11), and, if a comparison is made between equation (C.11) and equation (C.12), one can see that protein adsorption is Langmuirian only if ν approaches unity and $\phi_p \ll 1$.

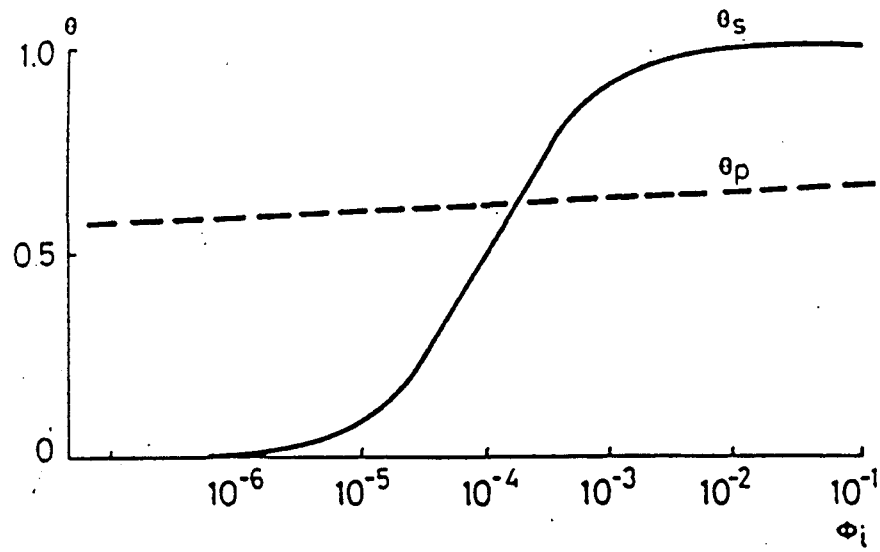

Figure C.1 Theoretical adsorption isotherms of a surfactant (θ_s) and a polymer (θ_p) as given by Eq (C.10) and (C.12). ΔE_s = -12kT, ΔE_p = -60kT, and ν = 50. *Source: ref. 6.*

Figure C.1 shows the adsorption isotherm of a surfactant as given by equation (C.10) and of a polymer as given by equation (C.12). The adsorption isotherm of the polymer exhibits a high affinity character, in other words, high adsorption at very low bulk concentration and a plateau almost over the entire range.

Levine (7) studied thermodynamics of adsorbed protein films. A schematic representation of an adsorbed film is shown in Figure C.2.

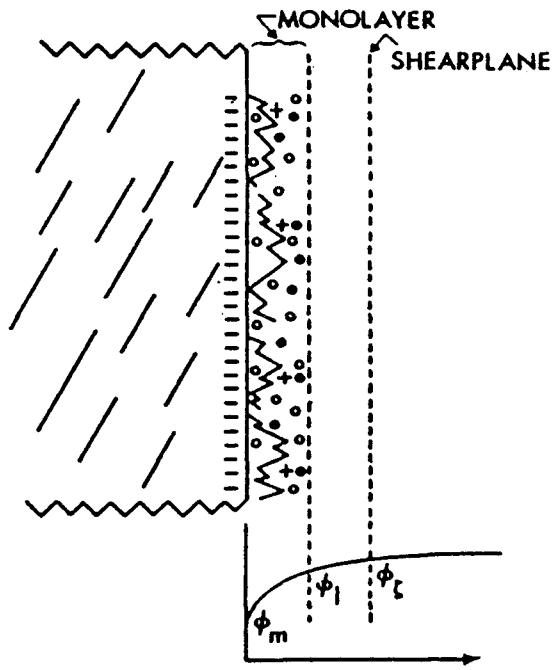

Figure C.2 A schematic diagram shows a negative surface with adsorbed monolayer of protein (wavy line), counter ions, and solvent molecules together with the various potentials. *Source: ref.* 7.

The film consists of adsorbed protein, counter ions, and solvent. The electrostatic potential at the surface-protein interface is denoted by ϕ_m, that at the protein-liquid side interface by ϕ_1, and that at the shear plane by the zeta potential, $\phi\zeta$. Such potentials are measured with reference to the bulk phase. For simplicity, the adsorbed film was assumed to consist of n_p^m moles of protein with molecular charge z_p, n_c^m moles of counter ions with ionic charge z_c, and n_s^m moles of solvent with zero charge. The same notation will be adopted for the bulk phase but without the superscript m. The subscripts p, c, and s denote protein, counter ion, and solvent, respectively.

If the protein p binds with ν sites at the surface in exchange with s solvent molecules, the following equilibrium is set up:

$$P + \nu S^m \rightleftharpoons P^m + \nu S$$

The equilibrium constant K would be:

$$K = \frac{a_p^m}{a_p}\left(\frac{a_s}{a_s^m}\right)^{\nu} \tag{C.13}$$

expressed in terms of the activity coefficients, it becomes:

$$K\,\frac{f_p(f_s^m)^{\nu}}{f_p^m(f_s)^{\nu}} = \frac{\bar{n}_p^m(C_s)^{\nu}}{C_p(\bar{n}_s^m)^{\nu}} \tag{C.14}$$

where $\bar{n}_p^m$ is the protein surface concentration [moles per unit area]; and $\bar{n}_s^m$ is the solvent surface concentration [moles per unit area].

For a dilute system, $f_i = 1.0$

$$K = \frac{\bar{n}_p^m (C_s)^\nu}{C_p (\bar{n}_s^m)^\nu} \tag{C.15}$$

If the internal energy, Helmholtz, and Gibbs free energies are denoted by U, F, and G respectively, they can be defined as follows:

$$dU' = T\,dS' - P\,dV' + \gamma dA + \Sigma \mu_i' \, dn_i' \tag{C.16}$$

$$F' = U' - TS' \tag{C.17}$$

$$G' = F' + PV' - \gamma A \tag{C.18}$$

$$G' = \Sigma \, n_i' \mu_i' \tag{C.19}$$

where the prime superscript denotes a total system property (i.e., bulk plus surface phase), μ_i the electrochemical potential of the i^{th} species, A the area of of the interface, and γ the interfacial tension. The quantities F′and G′ can each be split into a surface component which depends on both n_i and n_i^m, and a bulk phase component which depends on n_i only, thus:

$$F'(T,V,\gamma,n_i^m,n_i) = F(T,V,n_i) + F^m(T,V,\gamma,n_i,n_i^m) \tag{C.20}$$

$$G'(T,P,\gamma,n_i^m,n_i) = G(T,P,n_i) + G^m(T,P,\gamma,n_i^m,n_i) \tag{C.21}$$

Taking the partial derivative with respect to n_i^m yields

$$\left(\frac{\partial G'}{\partial n_i^m}\right)_B = \left(\frac{\partial G^m}{\partial n_i^m}\right)_B = \left(\frac{\partial F^m}{\partial n_i^m}\right)_B + PV_i^m - \gamma A_i \tag{C.22}$$

where B stands for the set of independent variables $\{T,P,g,ni,n_j^m\}$, and V_i^m and A_i are defined by the following relationships:

$$V_i^m = \left(\frac{\partial V^m}{\partial n_i^m}\right)_B \quad \text{and} \quad A_i = \left(\frac{\partial A}{\partial n_i^m}\right)_B \tag{C.23}$$

By defintion, the chemical potential is defined as:

$$\mu_i^m = \left(\frac{\partial G^m}{\partial n_i^m} \right)_B \tag{C.24}$$

At equilibrium, the film and bulk phase chemical potentials are equal.

$$\mu_i = \mu_i^m = \left(\frac{\partial F^m}{\partial n_i^m} \right)_B + PV_i^m - \gamma A_i \tag{C.25}$$

For low concentrations of protein, Helmholtz free energy of the film can be defined as if it was for an ideal bulk phase solution, thus:

$$F^m = G^m - PV^m = \Sigma \, (\mu_i^m - PV_i^m) n_i^m \tag{C.26}$$

For an ideal solution, the chemical potential is defined as:

$$\mu_i^m = \mu_i^{om} + RT \ln X_i^m + Z_i F \phi_m \tag{C.27}$$

Substituting equation (C.27) in equation (C.26), then taking the partial derivative with respect to n_i^m yields:

$$\mu_i^o + RT \ln X_i = \mu_i^{om} + RT \ln X_i^m - \gamma A_i^m + Z_i F \phi_m \tag{C.28}$$

The standard states for both the protein and solvent are:

$$\gamma_{op} A_p^m = \mu_p^{om} - \mu_p^o \tag{C.29}$$

$$\gamma_{os} A_s^m = \mu_s^{om} - \mu_s^o \tag{C.30}$$

Resolving equation (C.28) into its components (i.e., the solvent and protein) and using the standard states described in equations (C.29) and (C.30), one gets:

$$RT \ln \left\{ \frac{X_s^m}{X_s} \right\} = (\gamma - \gamma_{os}) A_s \tag{C.31}$$

$$RT \ln\left\{\frac{X_p^m}{X_p}\right\} = (\gamma - \gamma_{op})\, A_p - Z_p F \phi_m \qquad (C.32)$$

Hence:

$$\frac{X_p^m}{X_s^m} = \frac{X_p}{X_s} \exp\frac{1}{RT}\left\{(A_p - A_s)\gamma + (\gamma_{os}A_s - \gamma_{op}A_p) - Z_p F \phi_m\right\} \qquad (C.33)$$

or:

$$q = \left[\frac{X_p^m / X_s^m}{X_p / X_s}\right] = \exp\frac{1}{RT}\left\{(A_p - A_s)\gamma + (\gamma_{os}A_s - \gamma_{op}A_p) - Z_p F \phi_m\right\} \qquad (C.34)$$

The quotient q, denoted as the enrichment factor of the film by protein, is usually greater than one, and in order to satisfy this condition, the following inequality should hold:

$$\left\{(A_p - A_s)\gamma + (\gamma_{os}A_s - \gamma_{op}A_p) - Z_p F \phi_m\right\} > 0$$

The following three constraints should be met as well: (1) the protein partial molar surface area (A_p) is greater than that of the solvent (A_s); (2) the interfacial tension of the pure solvent is such that $\gamma_{os} > \gamma_{op}(A_p/A_s)$; and (3) the surface and protein have opposite electrostatic charges.

The first constraint is easily satisfied since for proteins, in general, $A_p \gg A_s$. The second constraint addresses the importance of surface energetics since γ_{os} is directly related to the pure substrate surface energy; consequently, materials with high surface energy are expected to adsorb more than those of low surface energy. The third constraint demonstrates the role of electrostatic charge of either enhancing or minimizing the process of adsorption from the electrostatic

barrier point of view.

C.2 EXPERIMENTAL OBSERVATIONS

C.2.1 KINETIC STUDY

Horbett (8) studied the adsorption of plasma proteins at polyethylene, surface-grafted with methacrylate derivatives, using an I-125 radiolabelling technique. Measurements were taken after ten different plasma exposure periods from 0.5 to 240 minutes. He found that for hemoglobin the adsorbed amount generally increased with time, and varied from one surface to another. The adsorbed amount was observed to increase with increasing surface hydrophobicity. On all polymers, the amount present at the shortest contact time (0.5 min.) was very low (0.005 $\mu g/cm^2$) and only gradually increased, implying that the rate of adsorption of hemoglobin to surfaces from plasma is much lower than what diffusion would predict. Horbett suggested that this may be due to multilayer formation, enzymatic cross linking, interfacial aggregation, configurational rearrangements, or chemical alterations in the adsorbing species.

For albumin, which constitutes a high percentage of plasma proteins, he found that it reacts more rapidly than others on polyethyl methacrylate/polyethylene but finally is displaced by a more slowly reacting protein, e.g. hemoglobin.

De Feijter et al. (9) studied the adsorption behavior of synthetic and biopolymers at the air-water interface using ellipsometry. They

dealt with non-uniformity of biofilms by averaging both the refractive index and thickness over the entire adsorption distance (i.e., depth) according to:

$$\bar{n}_1=\int_0^\infty n_1(n_1-n_2)dz \;/\int_0^\infty (n_1-n_2)\,dz \tag{C.35}$$

and

$$\bar{h}_1=\int_0^\infty (n_1-n_2)dz \;/(\bar{n}_1-n_2) \tag{C.36}$$

where n_1 represents the film refractive index as a function of the adsorption depth and n_2 is the bulk refractive index.

Also, by assuming the refractive index of the film to be a linear function of the solute concentration in accordance with the following equation:

$$n_1=n_2+a\Delta c_1 \tag{C.37}$$

where $\Delta c_1=c_1(z)-c_2$ is the excess concentration of the solute in the adsorbed layer (mass per volume unit), $c_1(z)$ is the absolute concentration in the layer, c_2 is the solute concentration in the bulk solution (i.e., at $z=\infty$), $a=dn/dc$ is the (ca. 0.18 ml/g) is the refractive index increment of the solute, the adsorbed amount can be expressed as follows:

$$\Gamma=\int_0^\infty \Delta c_1 dz \;=\frac{\int_0^\infty a\Delta c_1 dz}{a} \;=\frac{\bar{h}_1(\bar{n}_1-n_2)}{a} \tag{C.38}$$

where Γ is the adsorbed mass (mg/m^2), and $\bar{h}_1$ and $\bar{n}_1$ are obtained, using an iterative technique, based on the given optical properties of the

system (i.e., air-water interface with and without the film), and the wavelength and angle of incidence of the light beam.

De Feijter et al. (9) tested the adsorption of BSA, κ-casein, β-lactoglobulin, lysozyme and polyvinyl alcohol. Some of their experimental results are shown in Figures C.3 and C.4 and Table C.1.

For κ-casein, after an adsorption period of four hours and at low surface concentrations ($\Gamma \leq 2.5$ mg/m^2), the film thickness was found to decrease while the adsorbed amount still increased indicating a conformational rearrangement of the adsorbed molecule. The κ-casein molecules in solution are 5 nm in diameter, and the plateau values of the film thickness and adsorbed amount are 15 nm and 6.9 mg/m^2 respectively, indicating that a multilayer film was formed.

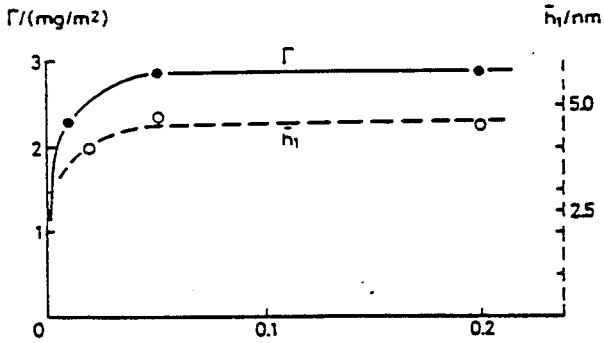

Fig. C.3 Surface concentration, Γ, and layer thickness, $\bar{h}_1$, for BSA as a function of protein concentration (pH = 6.7, IS =0.01 Eq/L, T = 23 ^{o}C). *Source: ref. 9.*

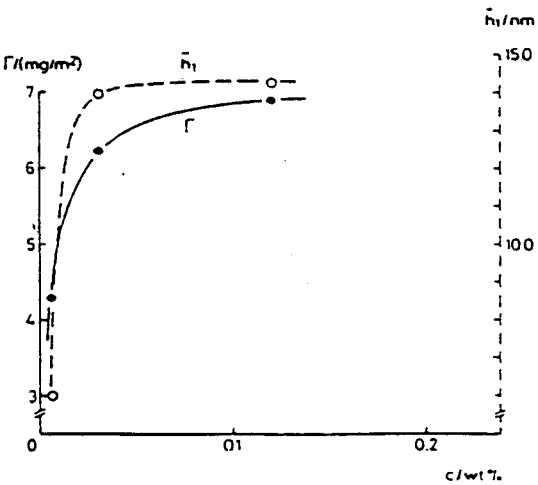

Fig. C.4 Surface concentration, Γ, and layer thickness, $\bar{h}_1$, for κ-casein as a function of protein concentration (pH = 6.7, IS =0.01 Eq/L, T = 23 ^{o}C). *Source: ref. 9.*

Table C.1 Ellipsometric parameters, $\partial\psi$ and $\partial\Delta$, excess protein concentration in adsorbed layer, Δc_1, thickness of adsorbed layer, $\bar{h}_1$, and surface concentration, Γ, of 8 x 10^{-5} Wt % solution of κ-casein.

t/h	$\delta\Delta$ (±0.02°)	$\delta\psi$ (±0.003°)	Δc_1 (g/ml)	$\bar{h}_1$ (nm)	Γ (mg/m^2)
0.16	1.08	0.000	>0.03	<9.0	0.20 ± 0.04
0.50	2.17	0.003	>0.07	<7.0	0.44 ± 0.06
1.00	3.67	0.008	0.04 ± 0.25	3.5 ± 2.5	0.75 ± 0.07
2.16	5.78	0.018	0.31 ± 0.08	4.2 ± 1.3	1.19 ± 0.06
3.42	7.13	0.029	0.29 ± 0.06	5.4 ± 1.3	1.51 ± 0.05
4.00	7.60	0.032	0.31 ± 0.06	5.4 ± 1.2	1.63 ± 0.04
21.0	9.93	0.041	0.62 ± 0.12	3.2 ± 0.6	1.89 ± 0.04

Source: ref. 9.

For polyvinyl alcohol, De Feijter et al. (9) found that the adsorbed amount was initially high then slowly decreased before it leveled off after one day. They attributed the overadsorption that occurred initially to the rate of adsorption (i.e., rate of diffusion) being considerably faster than the rate of conformational rearrangement. However, upon rearrangement some of the initially adsorbed molecules are "squeezed" back into solution. This event of overadsorption was not observed at low bulk concentrations; the rate of adsorption was apparently quite comparable with rate of conformational change.

C.2.2 NATURE OF ADSORBED FILM OF PROTEIN

Baier (12) investigated the initial events associated with interactions of blood with a foreign surface using three different techniques. Fresh flowing blood from lightly anesthetized dogs was

contacted with both germanium prisms and polymethylmethacrylate (PMMA) windows. After a desired period of exposure, the plates were rinsed, dried and later analyzed by multiple attenuated internal reflection (MAIR) infrared spectroscopy, ellipsometry and contact angle techniques.

A MAIR infrared spectrum is shown in Figure C.5 for a film formed after 5 seconds of contact with germanium. Diagnostic peaks for protein are seen with N-H bond absorption at about 3300 cm^{-1}, and the C=O stretch of the amide I and amide II bands at approximately 1650 cm^{-1} and 1550 cm^{-1}, respectively.

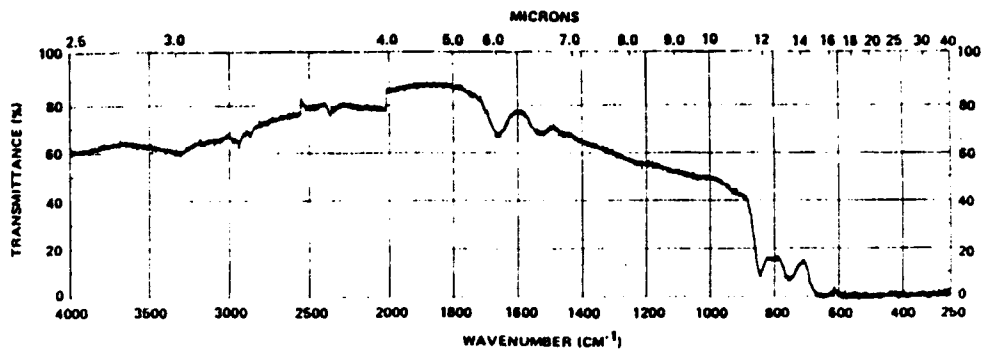

Figure C.5 A MAIR infrared spectrum for a film formed after 5 seconds of contact with germanium. *Source: ref. 12.*

Baier (12) suggested that the peak positions in the 1500-1700 wavenumber region suggest the presence of coiled protein conformations (e.g. α-helical, random tangle). From ellipsometric measurements, for the same exposure period, the average film thickness was about 50 Å (equivalent to two layers of stearic acid). A Zisman plot indicated a

critical surface tension of 36 dyne/cm on the film-covered surface. For a one minute exposure period, the MAIR spectrum was qualitatively similar to that of the five second film; however, the protein peaks were enhanced and a small absorption peak appeared at 1750 cm^{-1} suggesting inclusion of some fatty acid-like materials in the film. The average film thickness measured by ellipsometry was about 125 Å; the non-uniformity in the film thickness was more pronounced than that of the five second film.

Upon applying extraction to the one minute film, the CH_2 absorption band vanished, and the free carbonyl band disappeared completely. The protein bands remained, suggesting an irreversible adsorption associated with protein conformational rearrangement. It was only after mechanical scrubbing using a soft brush accompanied by an aqueous detergent solution, that the MAIR spectrum indicated a completely clean substrate, as also indicated from contact angle measurements.

Brash and Lyman (10) studied adsorption of plasma proteins in solution to uncharged, hydrophobic polymer surfaces using IR internal reflection spectroscopy. The polymer films used were low density polyethylene (LDPE), polystyrene, polydimethyl-siloxane, and fluorinated ethylene-propylene copolymer (Teflon FEP). The proteins used were albumin, γ-globulin, and fibrinogen. They studied the adsorption of plasma proteins under both static and flow conditions.

The adsorption isotherms on polyethylene at 37 ^{o}C are shown in Figure C.6, and the corresponding plateau values on different polymers are presented in Table C.2.

In general, the plateau values indicate a monolayer formation of protein at the surfaces, with the exception of γ-globulin on polydimethyl-siloxane which exhibited a more compact layer. The protein film thickness and the average area per protein molecule can be calculated from the data in Table C.2, given the molecular weight of each protein with the assumption that the density of adsorbing protein equals that of pure protein. The results are shown in Table C.3.

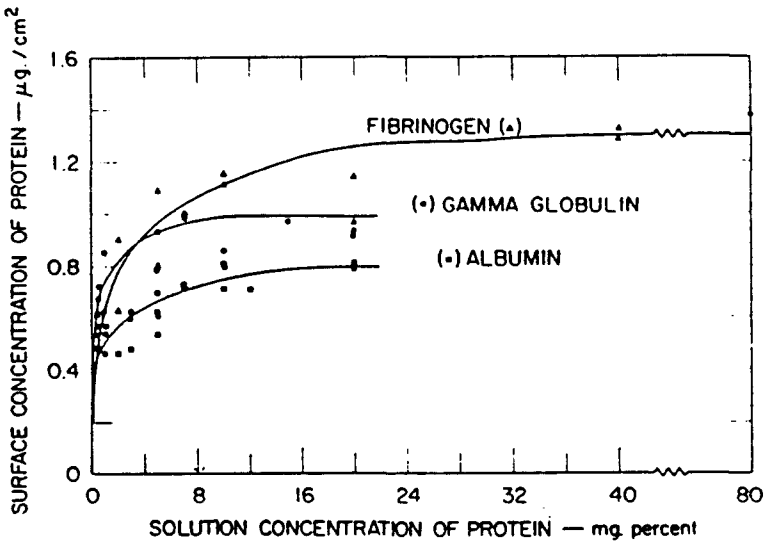

Figure C.6 Adsorption of plasma proteins to polyethylene at 37 °C. (Δ) Fibrinogen; (•) gamma globulin; (■) albumin. *Source: ref. 10.*

If the calculated thickness is compared with the dimensions of the native protein in solution, a "side-on" adsorption configuration is indicated, whereas the calculated area per molecule indicates an "end-on" configuration. Brash and Lyman (10) suggested the likelihood of "end-on" configuration as the molecular weight data is more reliable than the assumption of equal density among adsorbed and bulk protein.

In flow tests, Brash and Lyman (10) found that adsorption seems to be influenced only in the turbulent region. If the flow is laminar, the adsorption pattern appears similar to that of the static condition.

Table C.2 Surface concentration of plasma proteins adsorbed on polymer surfaces.

	Protein conc, $\mu g/cm^2$		
Polymer	Albumin	γ-Globulin	Fibrinogen
Polystyrene	0.5	0.7	1.7
Polyethylene	0.8	1.0	1.3
Silastic	1.6	1.8	1.6
Teflon FEP	0.8	0	1.4

Source: ref. 10.

Table C.3 Experimental dimensions of protein layers adsorbed on polymer surfaces.

Protein	Layer thickness, Å	Average area per molecule, $Å^2$
	on Polystyrene	
Albumin	44	2300
γ-Globulin	54	3800
Fibrinogen	130	4000
	on Polyethylene	
Albumin	62	1400
γ-Globulin	77	2660
Fibrinogen	96	5340
	on Silastic	
Albumin	120	720
γ-Globulin	138	1500
Fibrinogen	120	4200
	on Teflon FEP	
Albumin	62	1440
γ-Globulin	0	0
Fibrinogen	108	4760

Source: ref. 10.

C.2.3 THE EFFECT OF SURFACE ENERGETICS

Lee and Kim (42) studied the adsorption of proteins onto hydrophobic polymer surfaces. The proteins used in the investigation were albumin, γ-globulin, and fibrinogen and the substrate materials were poly(dimethyl siloxane) (SR), fluorinated ethylene/propylene copolymer (FEP), and a segmental copolyether-urethane-urea (PEUU). They studied protein adsorption under both static and flow conditions. The amount of adsorption was determined using internal reflection infrared spectroscopy (IRS). Some of their results are shown in Tables C.4, and C.5 and Figure C.7.

Table C.4 Protein adsorption to various surfaces.

Surface: Protein	Isotherm Plateau Bulk Conc. (mg%)	Plateau Time (min)	Plateau Conc. ($\mu g/cm^2$)	Rate Constant (min^{-1})
SR				
albumin	12	25	1.0	0.13
γ-globulin	25	30	1.3	0.15
prothrombin	15	10	2.3	0.67
FEP				
albumin	30	60	0.55	0.044
γ-globulin	30	60	0.80	0.083
prothrombin	30	25	0.85	0.19
PEUU				
albumin	15	25	4.5	0.11
γ-globulin	15	30	4.7	0.23
0rothrombin	15	10	4.7	0.38

Source: ref. 42.

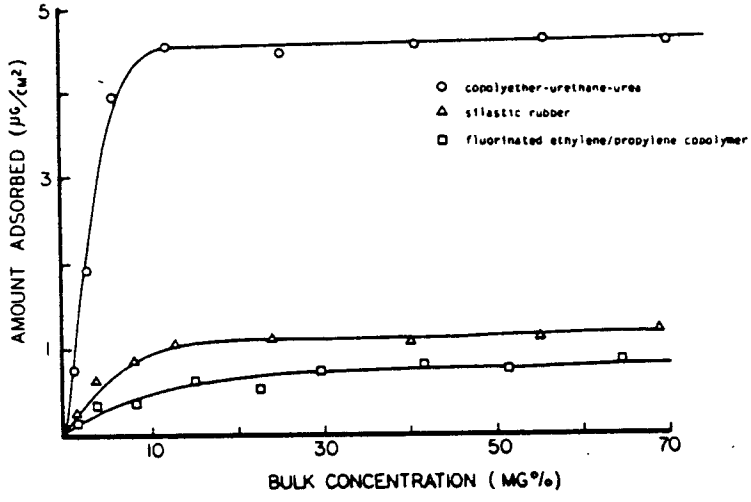

Figure C.7 Adsorption isotherms of albumin on selected polymer surfaces. *Source: ref. 42.*

Lee and Kim (42) found that adsorbed amounts of protein, plateau times, and adsorption rates depended upon the polymer surface, demonstrating the importance of hydrogen bonding and hydrophobic interactions, water structuring at the interface, and the configurational entropy of protein at adsorption sites.

They suggested that any one of the above mentioned factors could have explained the data; however, development of a comprehensive theory is difficult. Consequently, they suggested that proteins adsorbing on PEUU at higher rates and in greater amounts is mainly due to hydrogen bond formation.

In kinetic experiments, they found that by increasing the flow rate of the protein solution throughout their experimental set-up, the time required to reach a plateau increased since the shear forces opposed the diffusion of protein molecules toward the surface. Lee and

Kim (42) also found that the concentration required to reach the plateau depended upon the flow rate with SR but not with PEUU. This was explained by the fact that the SR surface is very rough relative to that of PEUU.

Table C.5 Protein adsorption to various polymer surfaces under flow conditions.

	Plateau Concentrations[a] and Plateau Times[b] at Flow Rates (in ml/sec) of:				
Surface: Protein	0	3	6	9	12
SR					
albumin	1.0	2.0	3.8	5.0	6.2
	(25)	(100)	(160)	(180)	(230)
γ-globulin	1.3	2.5	4.0	5.5	6.4
	(30)	(100)	(170)	(200)	(250)
prothrombin	2.1	3.7	4.9	6.4	7.3
	(10)	(70)	(140)	(180)	(200)
FEP					
albumin	0.6	1.1	1.4	1.6	1.8
	(60)	(60)	(70)	(70)	(60)
γ-globulin	0.7	1.1	1.6	1.8	2.0
	(60)	(70)	(70)	(80)	(80)
prothrombin	0.7	1.3	1.5	1.8	1.8
	(25)	(30)	(50)	(70)	(70)
PEUU					
albumin	4.4	4.6	4.5	4.7	4.6
	(25)	(40)	(100)	(155)	(170)
γ-globulin	4.7	4.6	4.8	4.7	4.8
	(30)	(50)	(100)	(150)	(190)
prothrombin	4.6	4.7	4.7	4.9	4.8
	(10)	(20)	(70)	(100)	(150)

a. Plateau concentration in μg/cm2.

b. Data in parentheses are plateau times in minutes.

Source: ref. 42.

Lee and Ruckenstein (11) studied the adsorption of proteins onto polymeric surfaces of different hydrophilicities. The materials used, with their properties described in parentheses are: (a) siliconized glass I (hydrophobic), (b) siliconized glass II (less hydrophobic than

type I), (c) PMMA (intermediate), (d) hydrogel I (hydrophilic), (e) hydrogel II (more hydrophilic than gel I), and (f) glass (high surface free energy).

Bovine serum albumin (BSA) was radiolabeled with ^{125}I. Small aliquots of labeled BSA were added to several 1 ml unlabeled BSA solutions of known concentrations and mixtures were contacted with the solid surfaces for 20 hours at room temperature. In adsorption kinetic experiments, samples were contacted with protein solutions for different periods of time. In other tests, surfaces were contacted with protein at different values of pH for 20 hours at room temperature, and also contacted with solutions of different ionic strength at pH 7.4. In all tests, the surfaces were preequilibrated with the appropriate buffer, and after adsorption the samples were rinsed by either one or both of the following methods: (1) gently rinsed until the radioactivity of the surface remained unchanged; and (2) immersed in 400 ml of fresh buffer until another constant radioactivity of the surface was attained.

As shown in Figure C.8, the maximum amount of adsorption occurred on the hydrophobic surfaces (solids (b) and (c)), and to a lesser extent on the hydrophilic surfaces (solids (d) and (e)). The most hydrophobic surface (solid (a)) exhibited an adsorbed mass smaller than either (b) or (c), and solid (f), the most hydrophilic, was comparable to solids (b) and (c).

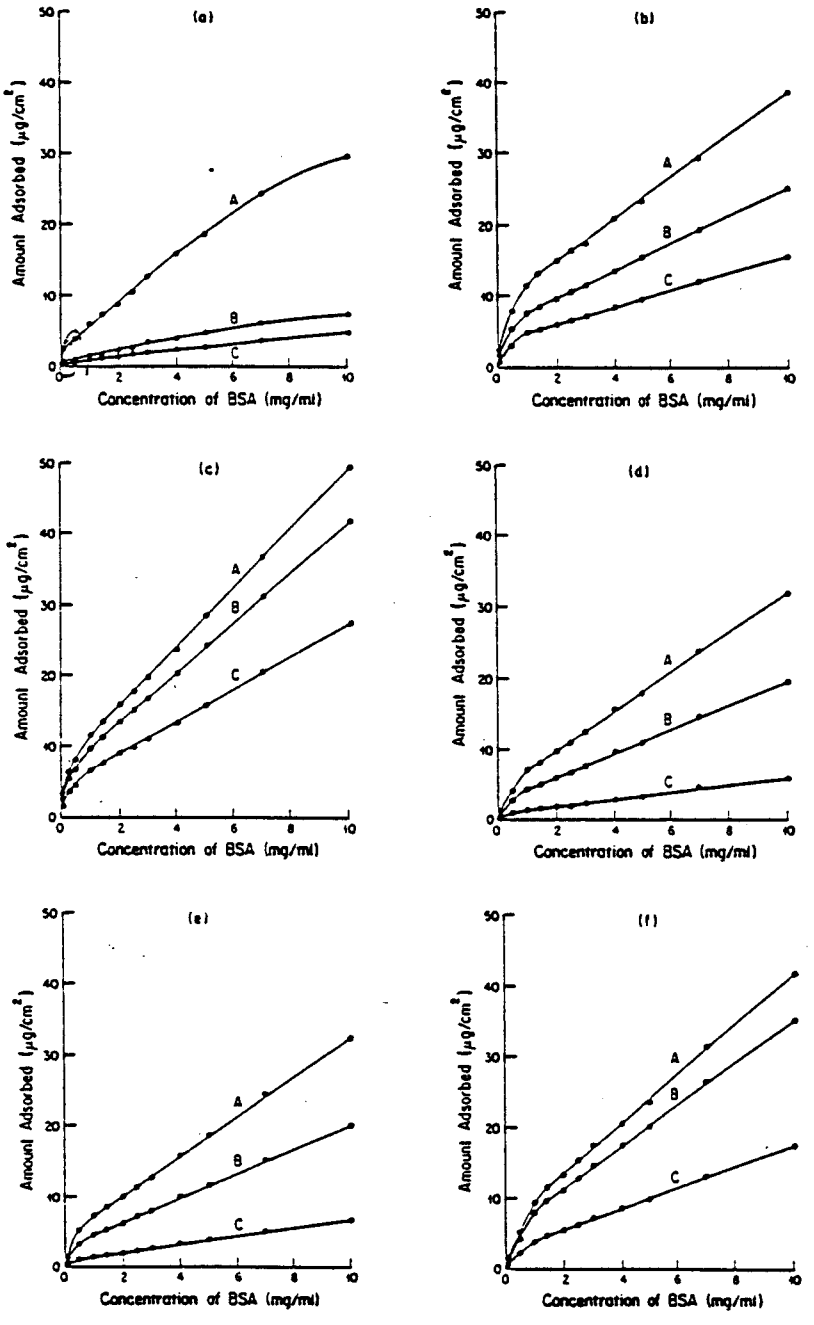

Figure C.8 Adsorption isotherms for BSA at 25°C on different surfaces. The total amount of adsorbed protein (A), and those remained adsorbed: 1. after rinsing with buffer until a constant value is reached (B), and 2. that after static desorption (C). *Source: ref. 11.*

Lee and Ruckenstein (11) evaluated a Hamaker constant specific for each surface; the Hamaker constant provides a quantitative indication of the strength of interaction between a protein molecule and a solid located in water, and Table C.6 shows the results of this analysis:

Table C.6 Estimated values of the Hamaker constant $A_{ps(w)}$ [joules].

Surfaces	$A_{ps(w)}$
Siliconized glass I	16.8×10^{-21}
Siliconized glass II	13.4×10^{-21}
PMMA	8.5×10^{-21}
Hydrogel I	0.8×10^{-21}
Hydrogel II	0.8×10^{-21}

ref. 11.

Solids characterized by high values of Hamaker constant are expected to exhibit greater amounts of adsorption than solids of smaller Hamaker constants. This criterion held true for solids (b) through (e); however, it did not hold for solid (a). Lee and Ruckenstein (11) explained this in terms of error associated with evaluation of the Hamaker constant for solid (a).

The effect of pH on the adsorbed amount is shown in Figure C.9. The maximum in adsorbed mass was observed to occur at pH values close to the isoelectric point.

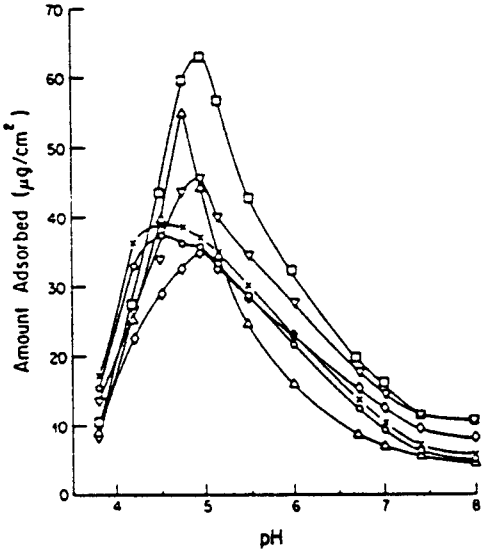

Fig C.9 Adsorption of BSA at room temperature on different adsorbent surfaces as a function of pH in acetic acid buffer. Siliconized glass I (Δ), siliconized glass II (fi), PMMA (∇), hydrogel I (O), hydrogel II (X), and glass (◊). *Source: ref. 11.*

Lee and Ruckenstein (11) attributed this to the globular configuration assumed by the protein at or around the isoelectric point, which would require minimal number of adsorption sites (footholds) needed for surface attachment. At pH values to the acidic or basic side of the isoelectric point, the protein configuration adopts a more extended form, and more surface sites (footholds) are needed to accommodate the same protein molecule relative to that needed for a globular configuration. In addition, the electrostatic double layer repulsion among the layers of adsorbed protein is enhanced, which results in a decrease in the adsorbed mass .

It is worth mentioning here that slight shifts noticed in the location of isotherm maxima with respect to the isoelectric point is evidence that protein adsorption is a function not only of the protein characteristics but also a function of surface energetics and microenvironmental conditions.

The effect of ionic strength on protein adsorption is addressed in Figure C.10. It shows that the adsorbed amount was observed to increase with increasing ionic strength up to a certain point where it leveled off. Lee and Ruckenstein (11) suggested that at low ionic strength (0.01 M), the dielectric permittivity of the medium is very high (i.e., coulombic interactions are more pronounced), promoting an extended form of protein configuration. This in turn results in a decrease in adsorbed mass from a foothold requirement standpoint. As the ionic strength increases, a shielding effect (effect of counterions) yields a more globular type of configuration, and electrostatics becomes a less important factor in the overall process.

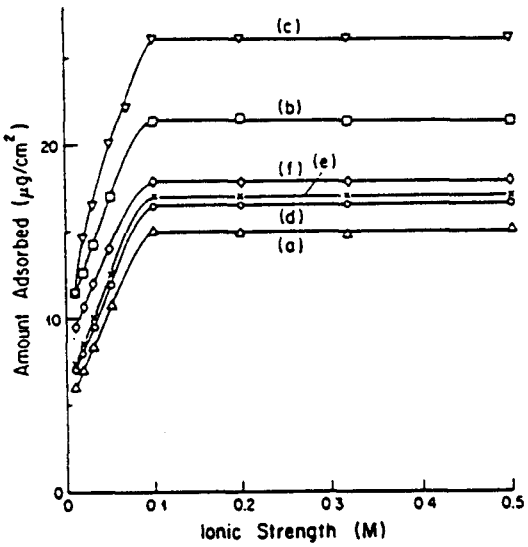

Figure C.10 Adsorption of BSA at room temperature on different adsorbent surfaces as a function of ionic strength in sodium phosphate buffer. Ionic strtengths were adjusted by addition of NaCl. (a) Siliconized glass I (Δ), (b) siliconized glass II (fi), (c) PMMA (∇), (d) hydrogel I (O), (e) hydrogel II (X), and (f) glass (◊). *Source: ref. 11.*

C.2.4 DESORPTION

Engström and Backström (18) examined detergency at hard surfaces using ellipsometry. They monitored adsorption of triglycerides and their removal by detergents from polyvinylchloride (PVC) and vacuum-deposited chromium glass. The triglyceride film was deposited on the surfaces by a spinning technique.

The adsorbed amount was determined based on the approach of Cuypers et al. (16) for ideal homogeneous films, where the adsorbed amount is expressed in terms of the specific density of the pure

protein, the volume fraction of the protein in the film, and the average film thickness. The PVC slides were examined to be smooth enough for ellipsometry. Some of their results are shown in Table C.7 and Figures C.11. The low values of film refractive index shown in Table C.7, in comparison to those of pure triglyceride, led Engström and Backström (18) to emphasize the importance of surface roughness rather than an optical property: i.e., n_f should be between the bulk refractive index, n_b, and that of pure triglyceride).

Table C.7 Average ellipsometer angle changes, film refractive index, film thickness, and triglyceride amount.

slide	$\Delta_{s+f} - \Delta_s$, deg	$\psi_{s+f} - \psi_s$, deg	n_f	d, nm	Γ_{McC}, $\mu g/cm^2$
		PVC (Grey)			
1% TP (11)[b]	6.03 ± 0.61	0.24 ± 0.11	1.415 ± 0.005	80 ± 6	3.6 ± 0.4
1% TO (6)	2.06 ± 0.52	0.10 ± 0.05	1.444 ± 0.019	33 ± 6	2.5 ± 0.3
2% TO (8)	4.47 ± 0.37	0.11 ± 0.12	1.413 ± 0.011	64 ± 4	3.7 ± 0.4
		Chromium			
1% TP (22)	−13.81 ± 0.49	5.45 ± 0.30	1.448 ± 0.007	55 ± 4	3.4 ± 0.2
2% TO (2)	−0.27 ± 0.06	0.51 ± 0.12	1.334 ± 0.001	151 ± 16	0.2 ± 0.1

TP: Tripalmitin, TO: Triolein.

Source: ref. 18.

The researchers made a comparison between the values of adsorbed mass on PVC obtained by a radioactive labelling technique and those obtained by ellipsometry. Ellipsometry was observed to yield an underestimate of adsorbed mass by 20% for triolein and an overestimate by 40% for tripalmitin relative to the values obtained by radiolabelling.

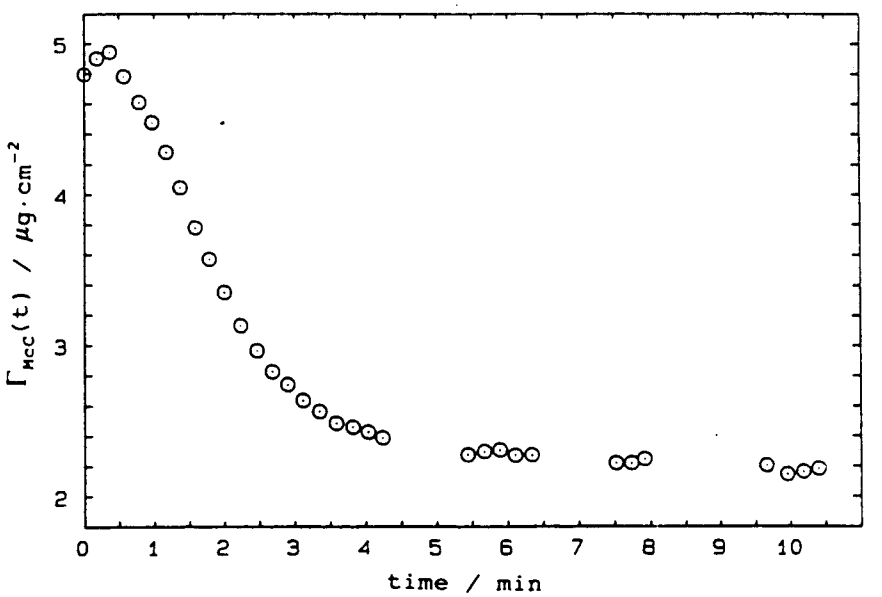

Fig. C.11 Removal of tripalmitin from a PVC surface by means of a non-ionic surfactant solution (0.04% (w/w) of pentakis(oxyethylene) dodecyl ether) vs. time. *Source: ref. 18.*

In summary, a great deal of effort has been devoted to studying the different factors that influence adsorption. The question of how these factors interact is undoubtedly complex, and a comprehensive model of protein adsorption is not available.